Ministry of Higher Education and Scientific Research
University of Baghdad
Institute of Laser for Postgraduate Studies

Holmium Emission Spectra Properties in Spectral Region (200-400) nm

A Thesis Submitted to the Institute of Laser for Postgraduate Studies, University of Baghdad in Partial Fulfillment of the Requirements for the Degree of Master of Science in Laser / Physics

By
Nibras Naziyah Mahmood

B.Sc. Laser Physics Sciences – 2002

Supervisor

Lecturer Dr. Mahmoad Shakir Mahmoad

2020 A.D **1441 A.H**

بسم الله الرحمن الرحيم

وَٱصۡبِرۡ لِحُكۡمِ رَبِّكَ

فَإِنَّكَ بِأَعۡيُنِنَاۖ

صدق الله العظيم

(سوره الطور ايه ٤٨)

Certification

I certify that this thesis was prepared under my supervision at the Institute of Laser for Postgraduate Studies, University of Baghdad, as a partial fulfillment of requirements for the degree of "Master of Science in Laser/ Physics Sciences".

Signature:

Name: **Dr. Mahmoad Shakir Mahmoad**

Title: **Lecturer**

Address: Institute of Laser for Postgraduate studies,
University of Baghdad.

Date: / / 2020
(Supervisor)

In view of the available recommendation, I forward this thesis for debate by Examining Committee.

Signature:

Name: **Asst. Prof. Dr. Hanan Jaafar Taher**

Title: Head of the Scientific Committee.

Address: Institute of Laser for Postgraduate studies,
University of Baghdad.

Date: / / 2020

Examination Committee Certification

We certify that we have read this thesis "In Line Fiber Pulse Compression" and as Examination Committee, we examined the student in its content and in our opinion, it is adequate with standards as a thesis for a degree of Master in science in Laser / Physics.

Signature:
Name: **Dr. Hanan Jaafar Taher**
Title: Assistant Professor
Address: Institute of Laser for Postgraduate studies, University of Baghdad
Date: / / 2020
(Chairman)

Signature:
Name: **Dr. Adi M.Abdul Hussien**
Title: Assistant Professor
Address: Applied Science Dept/ University of Technology
Date: / / 2020
(Member)

Signature:
Name: **Dr. Hassan N.Hashim**
Title: Assistant Professor
Address: College of Science/Al-NahrainUniversity
Date: / / 2020
(Member)

Signature:
Name: Dr. Mahmoad Shakir Mahmoad
Title: Lecturer
Address: Institute of Laser for Postgraduate Studies, University of Baghdad.
Date: / / 2020
(Supervisor)

Approval by the Deanship of Institute of Laser for Post graduate Studies, University of Baghdad.

Signature:
Name: Prof. Dr. Hussein A. Jawad
Title: Dean
Address: Institute of Laser for Postgraduate Studies, University of Baghdad
Date: / / 2020

I dedicate this work

To whom I bring his name proudly ...

My Father

To my eye light ... My mother

To my heart pulses ... My Brother and

Sisters

To everyone who helped me to do this work ……

Acknowledgment

At first, I thank ALLAH for everything because it pleased me things and make it easy. I would like to give special thanks to my supervisor **Dr. Mahmoad Shakir Mahmoad**, for suggesting this work, his guidance, encouragement and support have definitely had a substantial impact on this work. I have learned experimental techniques, numerical methods and theoretical analysis from him. I am greatly indebted to him for his constructive suggestions and criticism from time to time during the course of progress of my work.

My sincere gratitude and great appreciation to **Dr. Hussein Ali Jawad** Dean of Laser Institute for Postgraduate Studies, for his continuous support and crateful care during the period of search.

Many thanks to **Dr. Mohammed K. Dhahir** for his support and useful Advice.

Special thanks to **Dr. Ahmed Ismael Khaleel**, for his help and continuous support.

I highly appreciate **to Dr.Yosif Ibrahim Hammadi** for his support and useful Advice .

I would also like to thank all the faculty of Laser Institute for Postgraduate Studies who have been extremely helpful in the course of this project work.

Also I want to thank Engineer **Laith Tariq** for his assistance throughout the period of this work.

Finally, I would like to thank my family, specially my mother, my father and my brother **Firas** and sisters, **Marwa, and Zinah** for their patient and supporting me to the end.

Hopefully I didn't forget any body and if I did so I'm asking him to forgive me.

Nibras

Abstract

In this work, plasma emission spectra of the holmium target using Q-switched Nd:YAG laser (1064 nm) has been studied in the range of (200-400) nm region. Different laser pulse energies (600, 650, 700, 750 and 800) mJ with different repetition rate (1Hz, 5Hz, 10Hz and 20Hz) are used.

The influences of the laser pulse energy and pulse repetition rate on the emission lines intensity of the laser induced plasma spectrum by spectroscopic technique in air has been investigated. The best emission spectra appeared when the laser pulse energy is 800 mJ and 20 Hz repetition rate at λ= 341.54 nm, 342.76 nm, and 345.53 nm respectively with the maximum intensity of 80000 counts.

Holmium emission line intensities were studies for each individual emission for each line from λ = 342 nm to 349 nm with laser energy 650 mJ and 5Hz repetition rate. The maximum emission intensity line was 65535 counts appeared at ג = 345 nm. Also, the energy of each individual emission line from ג = 342 nm to ג = 349 nm was investigated in this work for the same laser energy 650 mJ and repetition rate of 5Hz. The maximum energy of line emission was 153 μJ at ג = 345 nm.

Cowan code was used to calculate the emission spectra probabilities for different transition of the holmium target.

The results indicate that, the emission line intensities increase with increasing of the laser pulse energy and repetition rate.

CONTENTS

List of Symbols

Symbols	Meaning
n_e	Electron number density
T_e	Temperature
B	Steady state magnetic field
n_i	Ion density
Z	Charge state
λ_D	Debye length
ϵ_0	Permittivity constant
K_B	Boltzmann constant
e	Electron charge
N_D	Number of electrons in Debye sphere
ω_P	plasma oscillation frequency
m_e	Electron mass
ω	Frequency of the electromagnetic wave
K	Propagation direction
c	Speed of light
n_c	Critical density

F_{Pond}	**Ponderomotive force**
I	**Field intensity**
E	**Electric field strength**
υ	**Frequency of the incident radiation**
ν_{ei}	**Electron-ion collision frequency**
γ	**Photon**
Z*	**Average ionization**
h	**Blanck constant**

Abbreviations

Symbols	Meaning
LPP	**Laser Produced Plasma**
LIP	**Laser Induced Plasma**
LTE	**Local Thermal Equilibrium**
CE	**Coronal Equilibrium**
CRE	**Collisional Radiative Equilibrium**
LIBS	**Laser Induced Breakdown Spectroscopy**

List of Contents

Chapter One

Introduction and Basic Concept

1.1 Introduction:

The plasma was defined as ionized gas. It's called fourth state for the matter because when heated the solid, the thermal movement of the atoms destroys the structure lattice of the crystalline, and formed liquid [1]. When sufficiently heated liquid to evaporate atoms from the surface faster than they recondense, gas is formed. Atoms collide with each other when gas was heated, and expel their electrons, then plasma was formed [2].

Plasma status is available more than the other states, that 99% of the universe in the case of plasma. Plasma is composed of positive charged ions, negative charged electrons, and neutrals atoms [3, 4]. The basic parameters to recognize the plasma are the electron number density (n_e), its temperature (T_e) and steady state magnetic field (B) [5]. Plasma is quasi-neutral which means the electron number density (n_e) and ion density (n_i) with charge state (Z) are balanced locally [6].

$$n_e = n_i Z \qquad (1.1)$$

The Debye shielding is an essential feature of a plasma which gives an example about collective behavior. It means that particles in plasma will be governed by the electromagnetic forces instead of collisions occurs in normal gas [7]. When charged particle is immersed inside the plasma, the potential around is shielded outside by either the ions or the electrons [8].

The Debye length (λ_D) is determined by the distance traveled [9], by charged particle in ½ π of plasma, and can be represented in this equation:

$$\lambda_D = \sqrt{\frac{\epsilon_0 K_B T_e}{n_e e^2}} \qquad (1.2)$$

Where (ϵ_0)was the constant of permittivity, (K_B) was the constant of Boltzmann, (T_e) was the temperature of electron, (n_e) was the plasma density, and (e) was the electron charge [7].

The concept of Debye length to be valid, it must have a number of charged particles (N_D) inside the Debye sphere. The number of particles in the Debye sphere can be described by [8]:

$$N_D = \frac{4\pi n_e \lambda_D^{\,3}}{3} \qquad (1.3)$$

Plasma frequency (ω_P) is afundamental parameter of plasma oscillation, and it's referring to the plasma frequency of electron (ω_{p_e}) due to the mass of ion is much larger and their oscillation is slower than the oscillation of electron . It is given by [9]:

$$\omega_{p_e} = \left(\frac{n_e e^2}{m_e \epsilon_0}\right)^{1/2} \qquad (1.4)$$

Where (m_e) was the electron mass, and (ϵ_0)was the permittivty in vacuum (8.854×10^{-12} F/m).

The wave of electromagnetic radiation (with frequency ω) propagates through the plasma depends on the density of electron. It is related to the dispersion relation which is given by:

$$\omega^2 = \omega_{p_e}^2 + c^2 k^2 \qquad (1.5)$$

Where (ω_{p_e}) is the frequency of the plasma, (k=2$\boldsymbol{\pi}$/λ) is the propagation direction, and (c) is the light speed [10].

When $\omega > \omega_p$, the electromagnetic wave is absorbed in plasma so (k) is real. For $\omega < \omega_p$, k is imaginary and the wave doesn't propagate through the plasma, and also if $\omega = \omega_p$, the reflection takes place, hence it is referred to the critical density where the density of plasma becomes so high and can be given by:

$$n_c = \epsilon_0 \, m_e \, \omega^2 / e^2 \qquad (1.6)$$

Where (m_e) was electron mass, and (e) was electron charge [11].

When propagate highly intense of laser pulse in gas, it will ionize the atoms partially or completely. Ionization leads to a continuous change in the density of electron throughout duration of laser pulse [12].

1.2 **Ponderomotive force**

The poneromotive force was averaged time force of particle charge oscillating in an electromagnetic (EM) field, was inhomogeneous spatially [13,14] .The ponderomotive force is given by:

$$F_{Pond} = \frac{e^2}{2\epsilon_0 m\omega^2} \nabla I(x) \qquad (1.7)$$

Where (m) was the particle mass, (e) was electron charge, (ϵ_0) was the permittivity in vacuum, and (ω) was the electromagnetic field frequency, and I(x) was the field intensity dependent-position.

The force of ponderomotive was formed as intensity gradient, and it’s directed toward low intensity area of the field [15,16]. The self-focusing was strongly dependent on the pulse width of the laser beam, and properties of the medium.

When an intense laser beam propagates through the plasma, this will lead to self-focusing[16]. This phenomenon is responsible among different processes nonlinear like ponderomotive, collisional, and relativistic nonlinearity. For intense and shorter laser pulses, these nonlinearities are dominant [17].

The relativistic nonlinearity is due to the mass of electron, and it is changed as the electron speed reached the light speed. In ponderomotive nonlinearity, the change on refractive index was arises because of the density variation induced by the force of ponderomotive [18]. For intense short laser pulse. The change on refractive index of plasma increases, and then decreases as laser pulse terminates. [19,20].

1.3 Laser Induced Plasma (LIP)

Laser induced plasma (LIP) was produced plasma by the laser interaction with mater when irradiance laser greater than a certain threshold [21]. Laser intensity (I) is proportional with the electric field as (E^2). The intense laser pulse produces electric fields which can remove electron from the solid target material by ionization and heating by collisions [22].Therefore, the intensity of the laser beam can be represented by [23]:

$$I = \frac{1}{2}\epsilon_0 c E^2 \qquad (1.8)$$

Where (I) was power density in (W/m^2), (c) was light speed (3×10^8 m/s), (E) was the strength of electric field (V/m) [24].

When the laser triggers the pulse, plasma will experience some conditions as a function of number density and temperature of species. In these conditions plasma is composed of ions, electrons, and neutral atoms [21].When an intense laser pulse focused on the solid target material, three processes are taken place.

First, the material ablation begins during the laser material interaction which causes heating and evaporation as laser pulse energy exceeds than the energy of ablation threshold for the solid target material [25,26]. In the initial stage of interaction, plasma began to be formed, as electrons escape from the solid surface by photoionization.

These electrons absorb laser radiation by inverse bremsstrahlung (IB) , So electrons are heated up and collide with the surface of the target, and more ionization will occur [27,28].

The process continues until the density of electrons becomes so high and reaches the critical density, and then the plasma frequency will be equal to the laser frequency. At this point, laser light can no longer reach the target, and reflected from the critical layer density. Subsequently, the plasma expands, and then the plasma density drops, and so the laser pulse once again can passes through plasma [28, 29]. The process is repeated again, when electrons are heated up by IB, and the density of plasma again increases to reach to the critical value. Figure (1.1) shows the interaction of intense laser pulse with a solid [29,22].

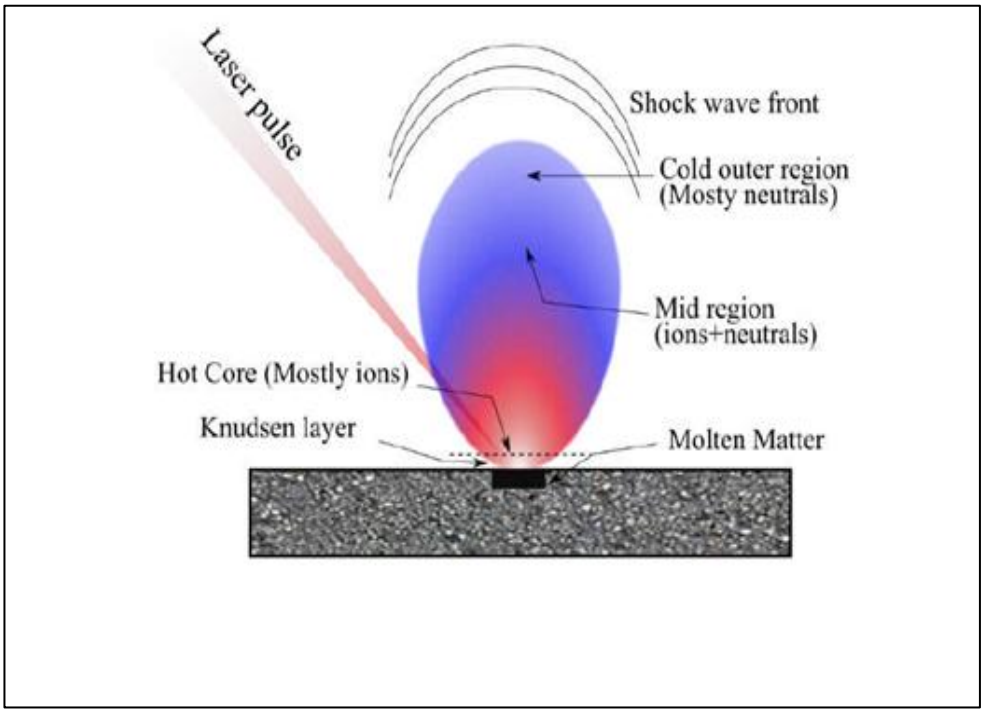

Figure (1.1): Schematic illustration of laser-induced plasma [30].

1.4 Atomic Emission Processes in Laser Produced Plasmas

There are three major mechanisms for the radiation emission in a partially ionized plasma, where the ions have not been stripped of all their electrons [27] . These mechanisms are:

1- bound-bound transition.

2- free-bound transition.

3- free-free transition.

1.4.1-Bound - Bound Transitions

This transition (between bond atomic states) can be observed in photo absorption (resonant absorption), and spontaneous decay. Photo absorption result by excited atoms from the ground energy levels to the higher energy level, and it is given by [29]:

$$e(E_1) + h\nu \longrightarrow e(E_2) \qquad (1.9)$$

Where $E_2 > E_1$ and $h\nu = E_1 - E_2$.

Inverse process (spontaneous decay) results by De- excited atom from higher energy levels to the ground energy levels, and can be represented by:

$$A^*(E_2) \longrightarrow A(E_1) + h\nu \qquad (1.10)$$

where $A(E_1)$ was the ground atomic state, $A^*(E_2)$ was the higher atomic states,(E1) was the electronic energy in the ground state , and (E_2) was the electronic energy in the higher state [31]. Figure (1.2**)** shows spontaneous decay and the inverse process, namely resonant absorption.

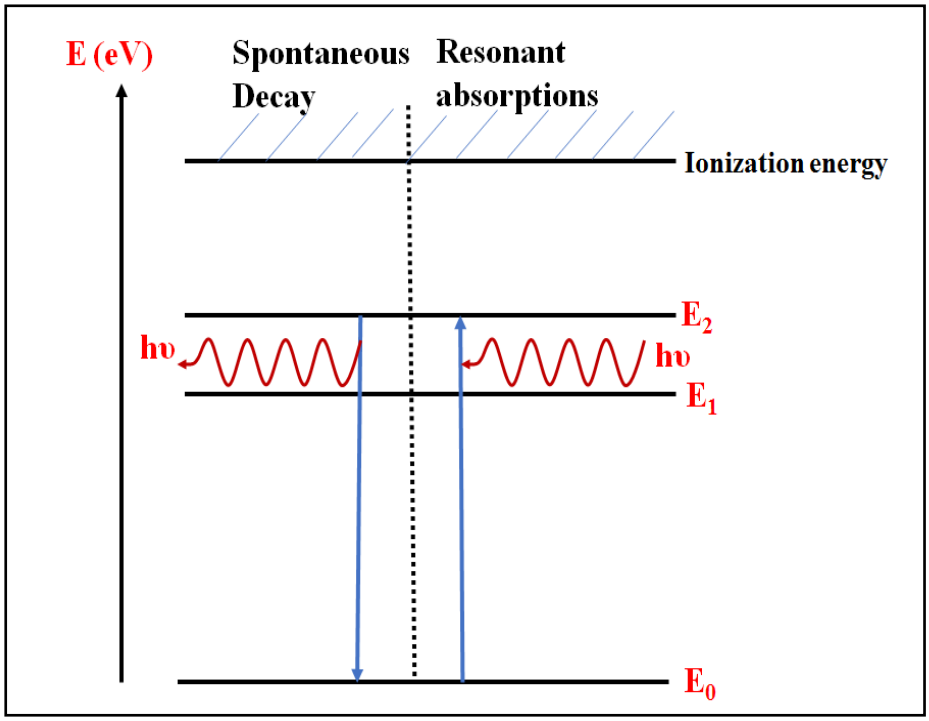

Figure (1.2): Resonant absorption and spontaneous emission [29].

1.4.2- Bound -Free Transitions

This process can be achieved when an ion captures free electron, the electron will emit its excess energy as a photon in recombination process ,and gives excess energy in the form of a photon [27,28]. The energy lost by the free electron in this process is represented as [29]:

$$e_1 + X^q \rightarrow X^{q-1} + h\nu \qquad (1.11)$$

Where (e_1) was free electron, (X^{q-1}, X^q) were charged successive ionic states, and (ν) was the frequency. Another process is photoionization , that take place when the energy of photon exceeds the ionization potential of the atom. The kinetic energy of the electron can be represented by [32].

$$E = \frac{1}{2} m_e v^2_e = h\nu - I_P \qquad (1.12)$$

Where (m_e) was the electron mass, (I_P) was ion or atom ionization potential, and (hv) was the photon energy.

The Photoionization process of photon absorption and break bound of electron, is given by:

$$h\nu + X^q \longrightarrow X^{q+1} + e^- (E) \qquad (1.13)$$

The Recombination and photoionization are shows schematically in Figure (1.3).

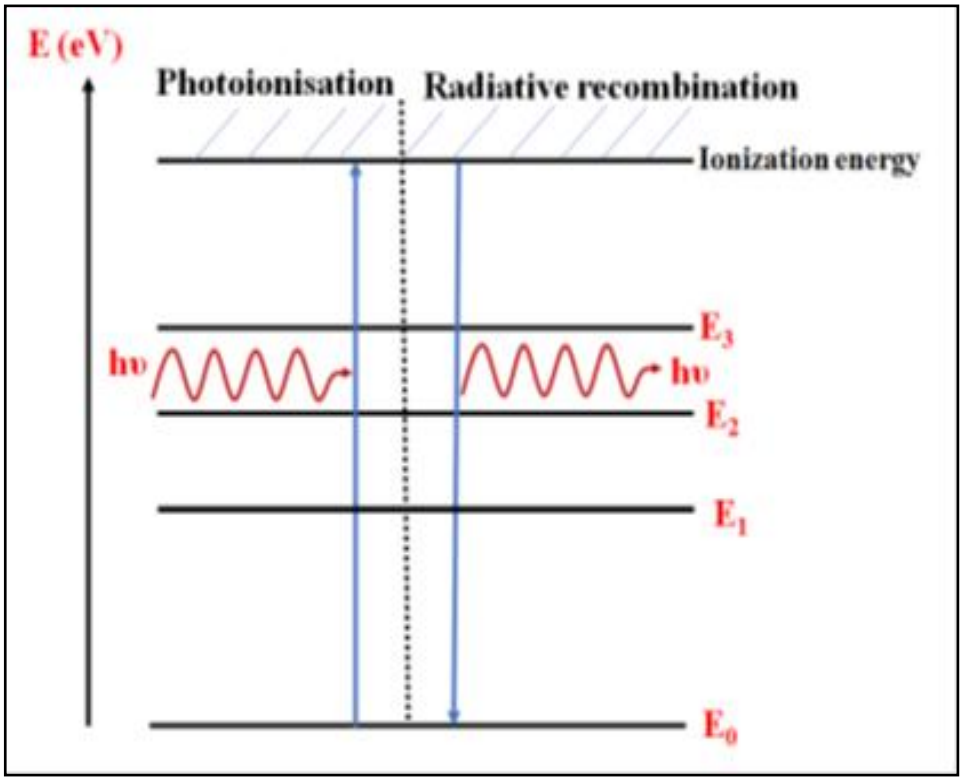

Figure (1.3): Photoionization and recombination processes [29].

Figure (1.4) shows afree electron captured by ion. It can break the bound electron in electron impact ionization process, and when ion counter two free electrons, one electron can be absorbed by the ion, and the others excess energy of electron gains in three body recombination process, was described by [23,28]:

$$e\,(E_1) + e\,(E_2) + X^{q+1} \longrightarrow X^{q+e}\,(E'_1) \qquad (1.14)$$

Where ($E1_{,}$ E_2) are the first and second state of electron kinetic energy, and (E'1) was the first state of electron kinetic energy by collision.

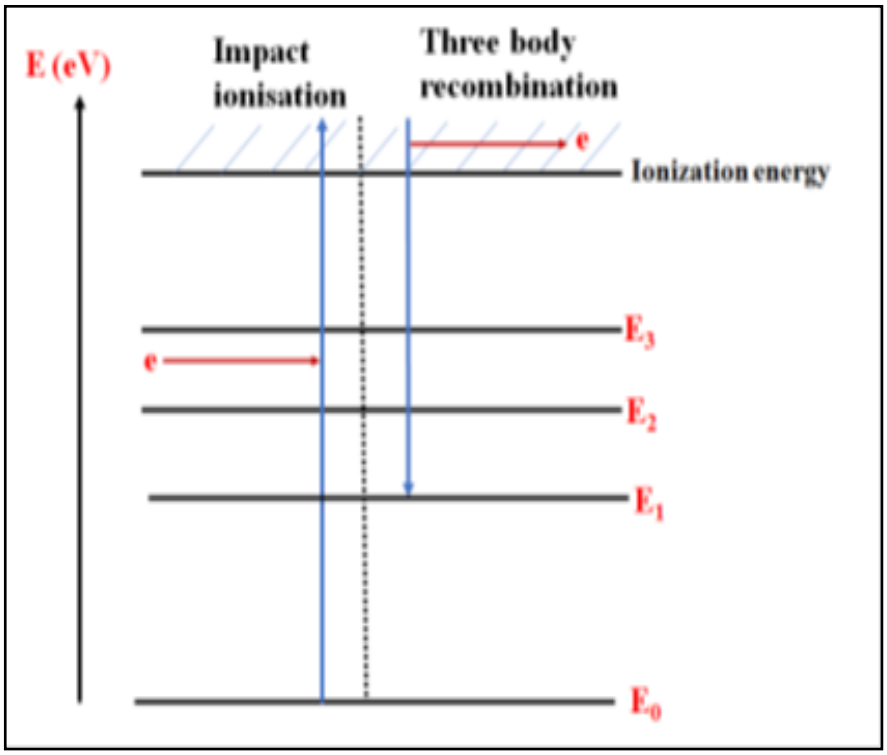

Figure(1.4): Electron impact ionization and three body recombination processes [28].

1.4.3- Free - Free Transitions

When a free electron was slowing down under the effect of an ion, the electron lost the kinetic energy excess, and emitted photon in a bremsstrahlung process. Which can shows in this equation [33]:

$$e_1\,(E_1) + X^q \longrightarrow X^q + e_1\,(E_2) + h\nu \qquad (1.15)$$

Where $E_1 > E_2$

The inverse process is possible. If a photon is absorbed by a free electron in the presence of ion resulting an increase in its energy in process inverse bremsstrahlung called,and can be described as [28].

$$e_1\,(E_2) + h\nu + X^q \longrightarrow e_1\,(E_1) + X^q \qquad (1.16)$$

Where, (X^q) was the neutral atom or ion, (E_1) and (E_2) was the energy of free electron after and before the interaction (inverse bremsstrahlung , bremsstrahlung).Figure (1.5) illustrates *bremsstrahlung* and *inverse bremsstrahlung* processes.

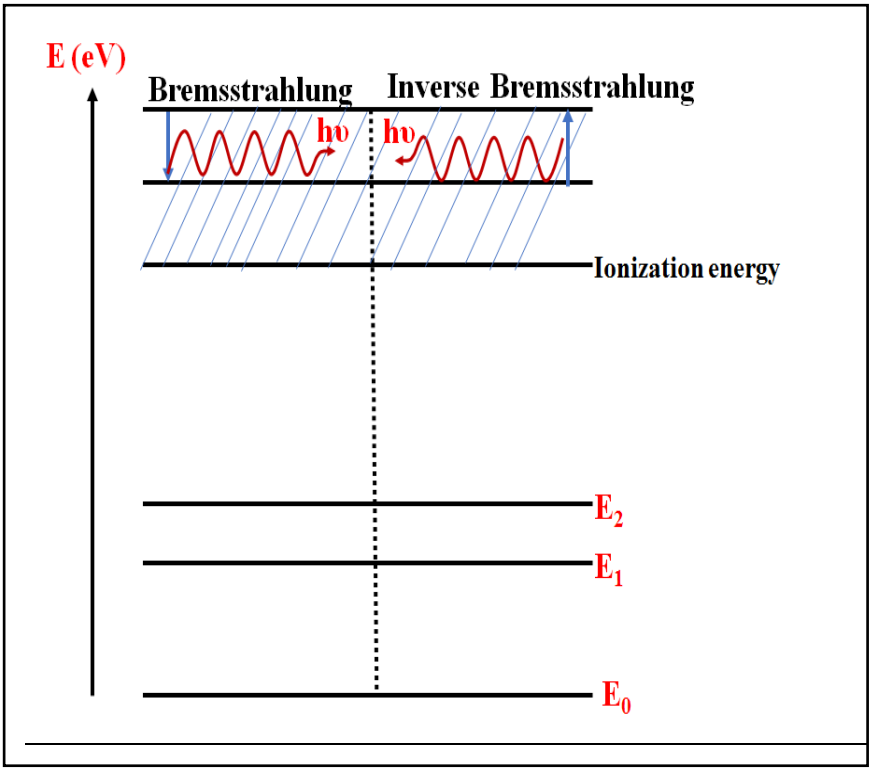

Figure (1.5): Bremsstrahlung and inverse bremsstrahlung processes [29].

1.5 Plasma Equilibrium

The most common equilibrium models used to describe plasmas are [34]:

1- Local Thermal Equilibrium (LET).

2- Coronal Equilibrium (CE).

3- The Collisional Radiative Equilibrium (CRE).

Figure (1.6) gives an idea about the range of validity of each model for a range of plasma densities and temperatures.

1.5.1- Local Thermodynamic Equilibrium (LTE)

In local thermodynamic equilibrium (LTE), the distribution of electrons densities are determined exclusively by particle collision processes (in optically thin plasmas), [35] which is dominate over radiative processes. The electron density must be high enough for the collision frequency to be high [36]. Local thermal equilibrium (LTE) is different from complete thermodynamic equilibrium in that the temperature need not be the same everywhere. The conditions that are required to achieve LTE are [37,38**]:**

1- The velocity distributions of ion and electron should follow a Maxwell-Boltzmann distribution**.**

2 – The dimensions of the plasma should be much smaller than the mean free path of the emitted photons but larger than the collision length of the electrons and ions.

3- The electron density should be high enough so that the ratio between collisional de-excitation and radiative decay should be larger than 10:1 for all transitions.

1.5.2- Coronal Equilibrium (CE)

The coronal equilibrium plasma, is described by high temperatures in the order of 10^6 K , and low electron densities (in the order of $10^8 c^3$) [35,39]. In (CE) plasma, with low electron density, and high temperatures optically thin .The atomic transitions that exciting transitions are collisional

between electrons and ions , and all de-exciting transitions are radiative occur by spontaneous emission [36].

1.5.3- Collisional Radiative Equilibrium (CRE)

This equilibrium describe intermediate regime of density (10^{19}-10^{21} cm^{-3}) .It lies between (LTE) plasma, and (CE) plasma [40]. It involves process of transition between excited level states which is caused by the electron collision. The plasma is assumed to be optically thin [41].

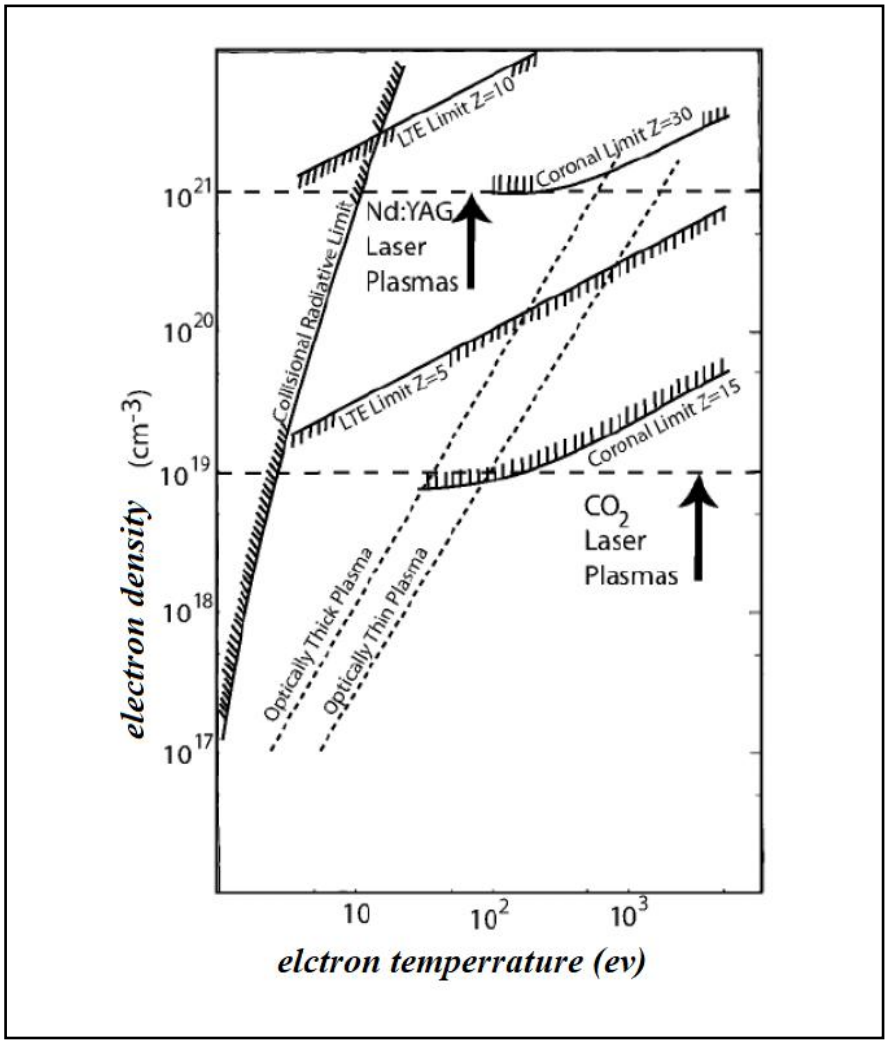

Fig.(1.6): The idea about the validity of each model for a temperatures and plasma densities [42].

1.6 Reactions in Plasmas

Excited atoms and ions produced different types of reactions in the plasma (Collision, Excitation Ionization, and Recombination)[43].Electrons in the plasma acquiring energy from the electric field, and collide with molecules of the gas [44].

The collisions of electrons caused ionization and excitation of the gas [45]. Recombination occurs when an electron is absorbed by ion, and the excess energy is emitted as a photons [46].The plasma produced by laser have high expansion velocities , high electron temperature (T_e), high electron density (n_e), and relatively high degree of ionization [47,48].

1.7 Plasma Expansion

The plumes of the plasma expansion start in the air and cool when the laser pulse terminates [49]. At the beginning of the plasma expand, the velocity of the electrons is greater than the velocity of ions [50], due to the relative mass difference[51]. At the plume front the electrons travel, and start to accelerate, leaves the ions behind far away from the bulk of the plasma. This causes a strong electrical potential to be created between the two species fronts. Figure (1.7) represented plasma plumes expansion.

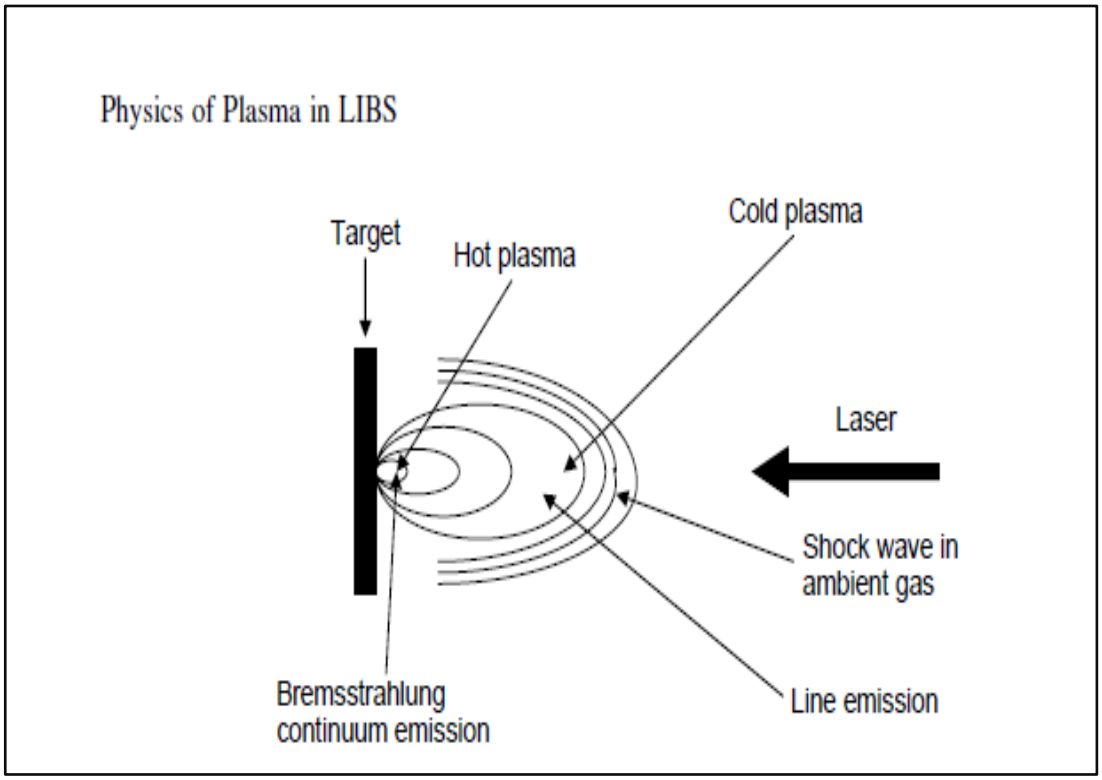

Fig (1.7): Schematic diagram of laser produced plasma expanding [50].

1.8 Plasma Lifetime

The plasma life time, as shown in fig (1.8) are divided into three stages:

1- Plasma ignition process and this process includes breaking the bond throughout the laser pulse, depending on the type of laser, radiation and pulse duration. [52].

2- The next stage the plasma is expand and cooling [53].

3- In the last stage of the life of the plasma the mass ablated are not excited as plasma or vapor , not emitted radiation . Ablated atoms becomes cold, and nanoparticles created by recombination process [54].

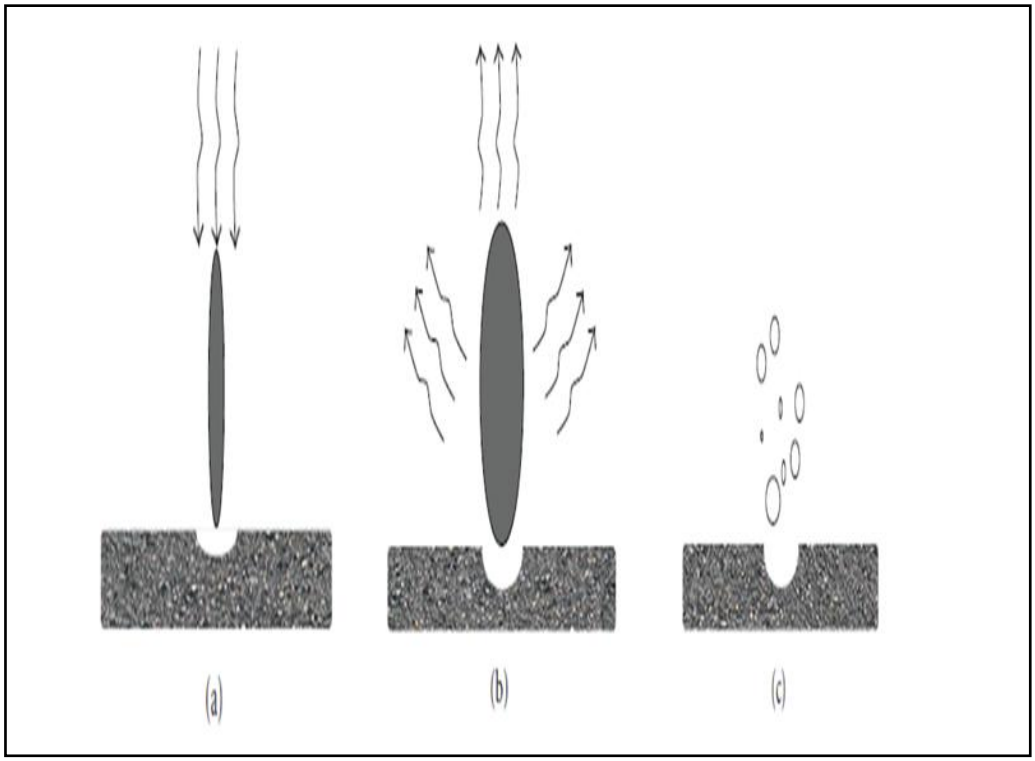

Figure(1.8) :Plasma life stages: (a) plasma ignition, (b) plasma expansion and cooling, and (c) particle ejection and condensation [52].

1.9 Fundamentals of Plasma Physics and Spectra

The plasma produced by intense laser pulse emitted light can give information about qualitative and quantitative analysis of the sample. Plasma emissions provided spectral signatures of many different type of materials in solid, liquid, or gas state [55].

Laser-matter interaction is governed by quantum mechanics laws that describe how photon is absorbed or emitted by atom [56].

If applied high energy to the atom greater than the ionization potential, electron expel from atom producing a free electron and positive ion [57]. Initially, the electron release from the atom is most external one (the furthest with respect to the nucleus), because it has the lowest ionization potential, but with higher energy applied there is a possibility to

escape more electrons , reaching to the second and the third ionization ,and so on [56]. The plasma emitted light consists of discrete line, band, and an continuum overlying [58].

The continuum emission of plasma is emitted as a result of free-free and free-bound transitions. The recombination process occurs when ion captures a free electron in a process called free-bound transition, or in the de-excitation process, the ions and the electrons lose energy due to kinetic process in a process called free-free transition [59].

Discrete lines are rise when the transitions accrue between atomic bound states. These lines appeared in both emission and absorption spectra, it is very important to characterized the material, three major features have such as shape, intensity and wavelength. This parameter depending on both the environment and structure of atom. Each type of atom has different energy level which determined the wavelength of the lines [58, 60]. Continuum radiation is very important to determine the parameters of plasma, such as density, pressure, temperature of electron, which are used to characterize the plasma [61, 57]. The whole process can be shown in Figure (1-9).

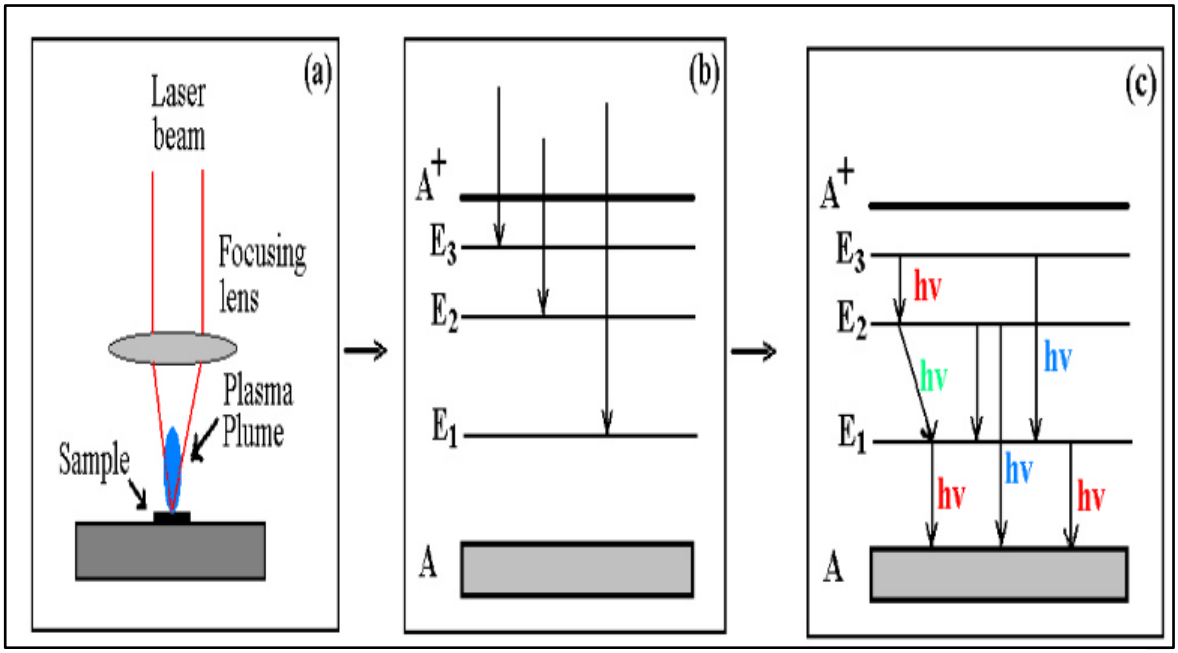

Figure (1.9): Timing of a LIPS process: (a) plasma ignition, (b) broadband emission due to Bremsstrahlung and free-bound transitions, (c) line emission due to bound-bound transitions [62].

1.10 Plasma Emission Spectra

Plasma emission line from atomic bond state may be hidden by continuum radiation that was causes by two processes. The initially was recombination process [63]. In this event, the electrons pass from the free State into the upper level bound of the ions, and fell down to the ionic ground state [64]. Second process (Bremsstrahlung process) is referred to the transitions free-free corresponding to the losses of kinetic energy by the electrons in the field of the ion.

When the electrons in the field of the ions their energy lost by deceleration process, then emit photon at different wavelength [65]. The continuum emission is strongly depends on both density and temperature of the plasma. [66].

1-11 Literature Review:

This review briefly describe, and shows some of previous results and researches of emission spectra of the plasma produce by laser interaction with solid target.

S. S. Harilal, et. al., in (1997), reported the spectra of C_2 plasma emission using laser Nd:YAG**.** The result investigated C_2 emission spectra intensity with the distance from the sample [67].

In (2000), Y. L. Chen, et. al., studied laser-induced breakdown and energy deposition in air, using Nd :YAG (1064 nm). The results of this work were compared with the predictions of the laser irradiance in the focal region. [68].

In (2001), B. Le Drogoff, et. al., characterized the plasma emission of Al, Mg by focusing a ultrashort laser pulses on them. The results of this work shows faster decay of continuum and line emission, shorter plasma lifetime than in case longer of laser pulse [69].

Rai, et. al., (2003), studied a plasma emission line intensity using doubled pulse Nd-YAG laser by atomic spectroscopic technique [70].

In (2005), S. S. Harilal, et. al., examined the plasma emission produced from tin target by focusing Q-switched Nd-YAG laser. The spectral data obtained from this work was plasma electron density [71].

N. M. Shaikh, et. al., (2007), discussed the spatial evolution of aluminum emission for plasma production, from three Q-switched Nd:YAG laser wavelengths (1064, 532, and 355) nm. The emission intensity of the spectral lines was stronger in the UV laser has been showed because of the higher ablation as compared to the visible and IR lasers [72].

In (2008). A. Elhassan, et. al., showed the influence of different laser pulse duration (nanosecond, and femtosecond), for emission spectra intensity from plasma induced at different elements (Pb, Zn, and Sn). It has been observed that the intensity of emission lines increases when a femtosecond laser pulses rather than nanosecond laser pulse [73].

In (2011) R. W. Coons, et. al., investigated Li plasma emission properties using Q-switched Nd:YAG laser. The results indicate that the intensity of plasma emission line depend on the laser source distance from the target [74].

M. Hanif, et. al., in (2013), examined titanium plasma emission properties using different wavelength of Nd:YAG laser (1064,and 532) nm, with different laser energies [75].

In (2014), a study for the influence of laser pulse energies for plasma emission line intensity of Zn target in air at atmospheric pressure was done **by H. Hegazy, et. al.,** their results were performed experiments at different laser energies and different delay times, which also allow us to study the dependence of the plasma evolution on the laser wavelength [76].

M. Hanif, and M. Salik, in (2015), characterized the properties of plasma emission at zirconium sample, were different wavelength of Nd-YAG laser and different energies are used. The researchers observed that temperature and number density increases as laser irradiance is increased. The temperature is also calculated by varying distance from the target surface along the line of propagation of plasma plume [77].

In (2017) Jiajia Hou, et. al., studied plasma parameters properties such as plasma temperature and electron density, by focusing Q-switched Nd:YAG laser at aluminum target, and the relationship between optically thin condition and plasma characteristics [78].

F. Torretti, et. al., in (2018), discussed the spectroscopic measuremens in the extreme ultraviolet (EUV) regime (7–17 nm) of molten tin illuminated by a high-intensity 3-J, 60-ns Nd:YAG laser pulse.The results resolve some long-standing spectroscopic issues and provide reliable charge state identification for Sn laser-produced plasma, [79].

Characterization the effect of laser pulse energy on Al and Cu plasma in air was done by **Qusay Adnan Abbas in (2019)**, using (1064nm) Nd:YAG laser with 6ns pulse width. It has been illustrated that the increasing of pulse laser energy causes to increase plasma emission line intensity [80].

1.12 Aim of The work

In this work, the aim is to study the properties of holmium emission spectra (experimentally and theoretically) for plasma produced by focused intense laser pulse at holmium target in order to get the emission spectra in the (200-400) nm region. Also the effect of laser parameters (laser pulse energy, and laser repetition rate) on the plasma emission spectra was investigated .

Chapter Two

Experimental Details

2.1 Introduction:

This chapter deals with the experimental set-up, and the technique which has been used during this work. Also deals with the theoretical code includes Cowan simulation code, which calculates the atomic structure of the holmium target.

2-2 The Experimental Set-up:

The experimental setup that has been used for obtaining the emission spectra of the plasma in the (200-400) nm region can be shown in figure ((2.1, a), (2.1, b)).

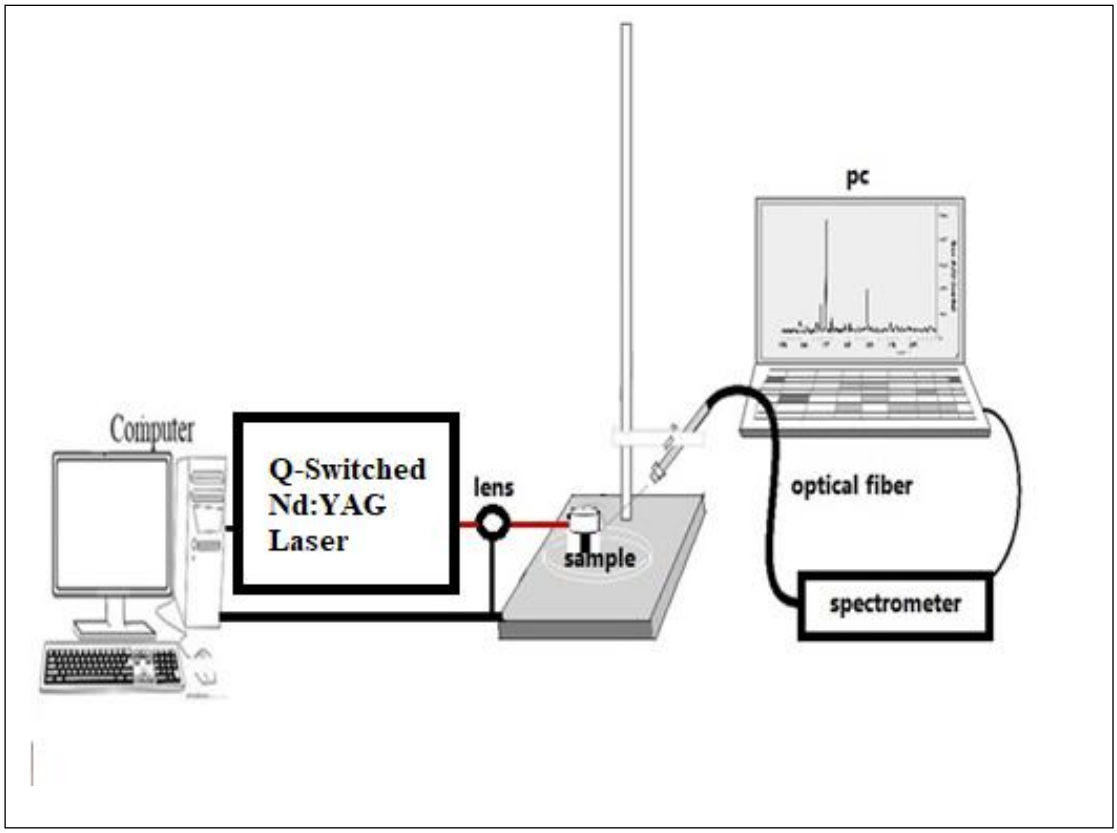

Figure (2.1 a): Schematic diagram of the experimental setup for laser induced plasma.

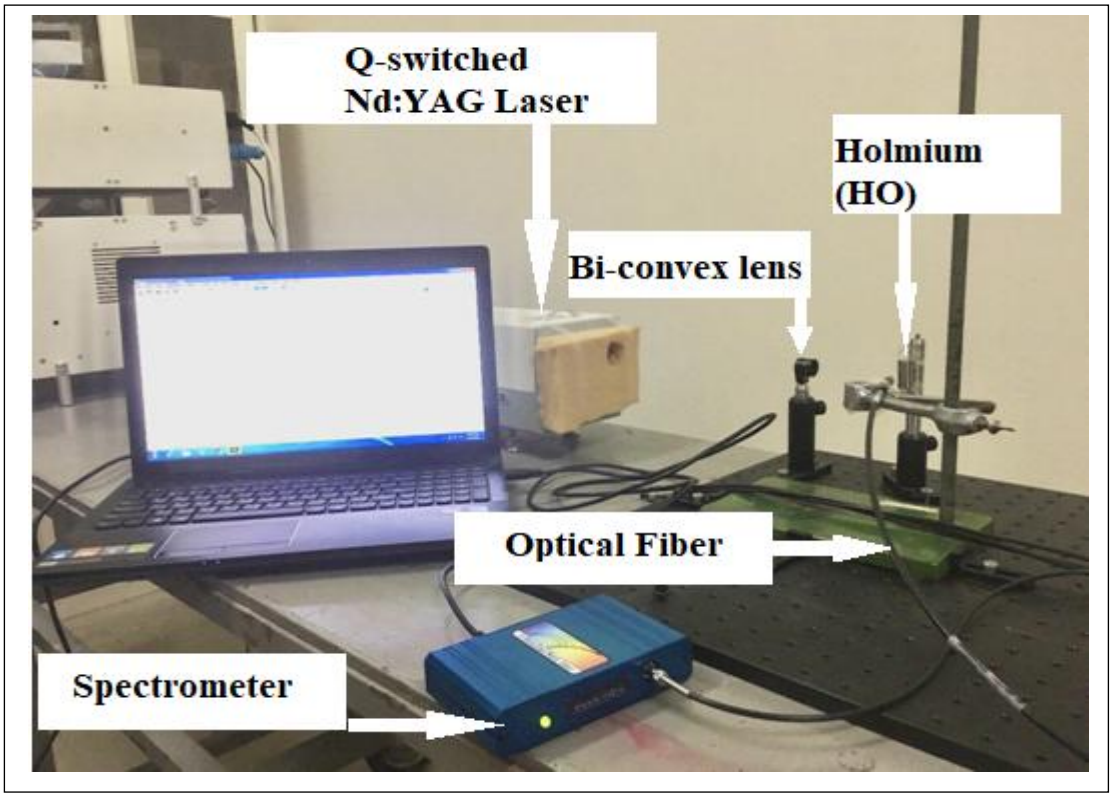

Figure (2.1b): The experimental setup

The experiment setup of this work is consisting of Nd:YAG laser, which is used to generate the plasma. This Q-switched Nd:YAG laser, generates a laser pulse width of (10 ns) with repetition rate of (1-20) Hz. The maximum energy of this laser pulse is 900mJ. This pulse is focused onto the surface of the target by a Bi-convex lens with 100 mm focal length. The distance from the target to the lens is about 100 mm. This lens is uses to get a spherical plasma plume and a reproducible breakdown. The plasma was formed in air at atmospheric pressure on 1.75mm^2 surface area of the solid target. The purity of the holmium rod was 99.9%. The emission was collected by the optical fiber which was set at an angle of about 45 degree from the target and diverted into a spectrometer which is connected to the laptop. To measure the intensity of each emission line at each wavelength, the following setup (as shown in figure (2.2)) was used.

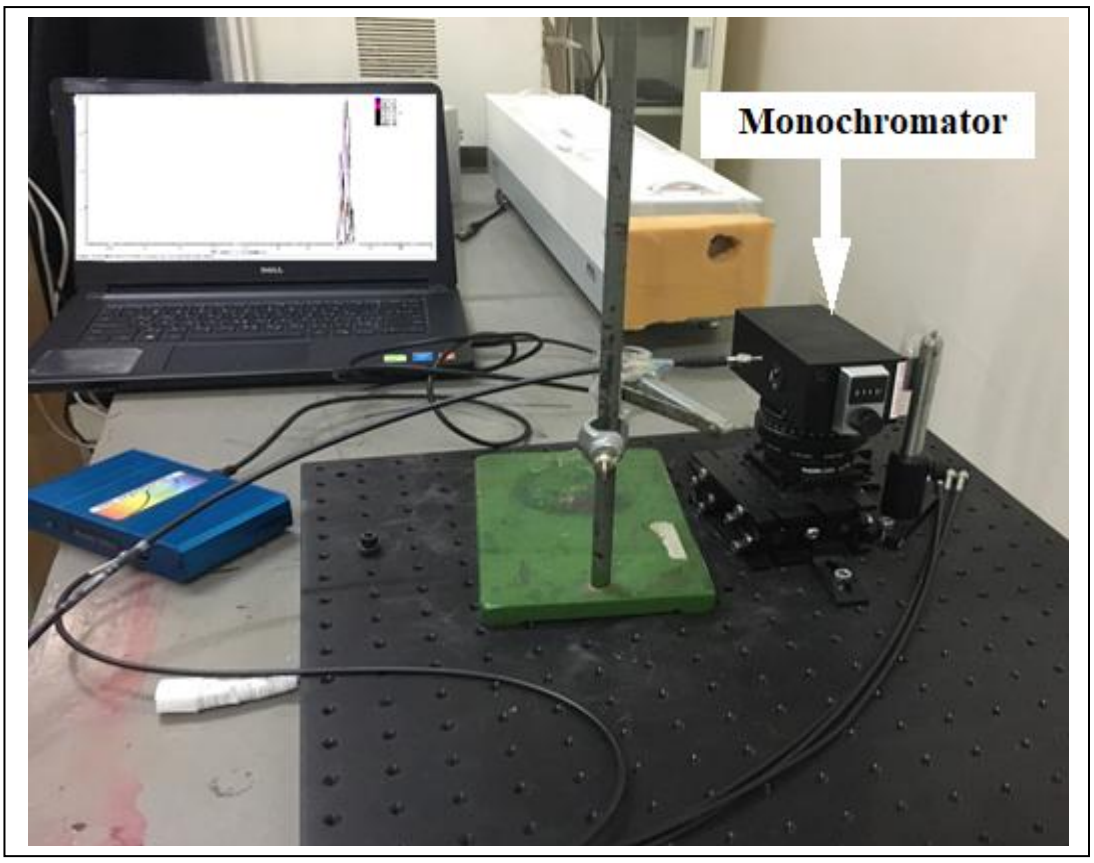

Figure (2.2): The experimental setup used to measure the intensity of each emission line

In this setup, the monochromator was set to different wavelength at each time, and shooting the focused Q-switched Nd:YAG laser pulse at holmium target in order to get the emission spectra .

To measure the energy of each emission line at each wavelength special energy meter device was used for this purpose. This setup is shown in figure (2.3).

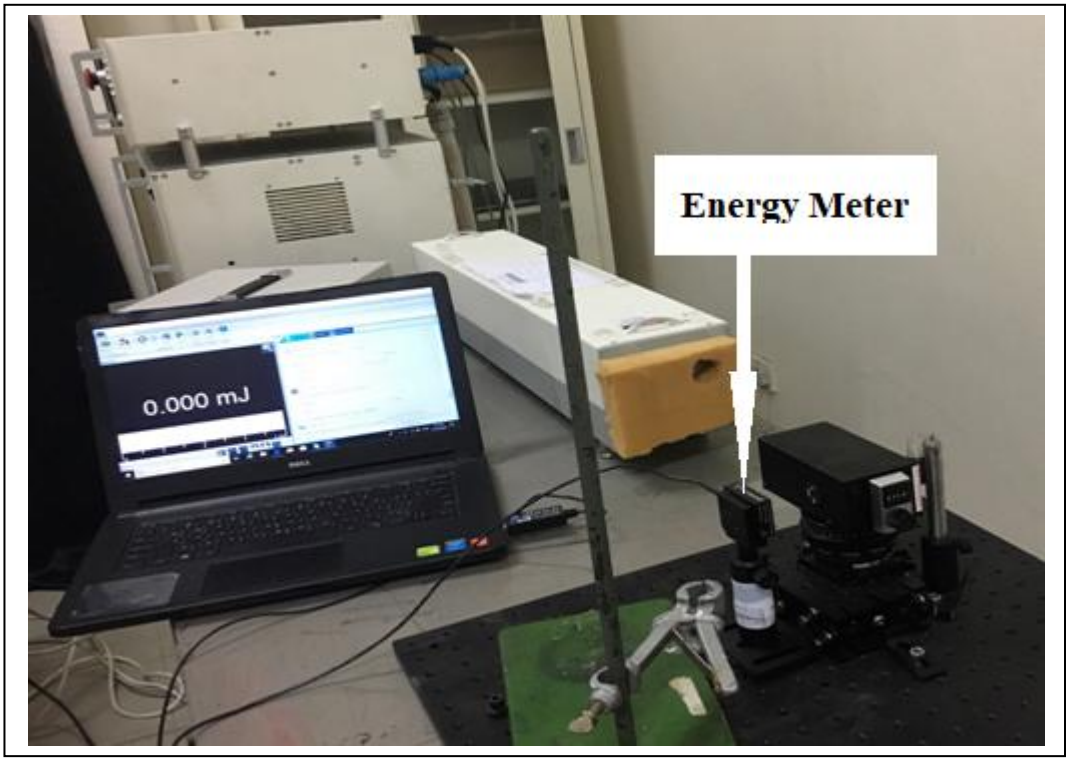

Figure (2.3): The experimental setup to measure the energy of each emission line

2.2.1 Nd:YAG Laser Source at 1064 nm

In this work, a pulsed Q-switched Nd:YAG laser, (model LF117, manufactured by SOL instruments with cooling system and power supply) was used as shown in Fig. (2.2, (a ,b, c)), and specifications of the laser source were listed in table (2.1) .

Figure (2.4): (a) Pulsed Nd: YAG laser LF117

(b) laser power supply, (c) cooling system.

Table (2.1): Specifications of the laser source.

Specifications	
Active medium	Nd:YAG
Wavelength	1064nm
Max.-Pulse energy	900mJ
Pulse width	10 ns
Pulse Repetition Rat	1- 20Hz
Beam Divergence	<0.7mrad
Beam diameter	~7.5 mm
Operating Mode	Pulse

2.2.2 Convex lens

A Bi-convex spherical lens (type LB1187-C-ML) manufactured by Thor Labs was used in this work. as shown in Fig. (2.5).

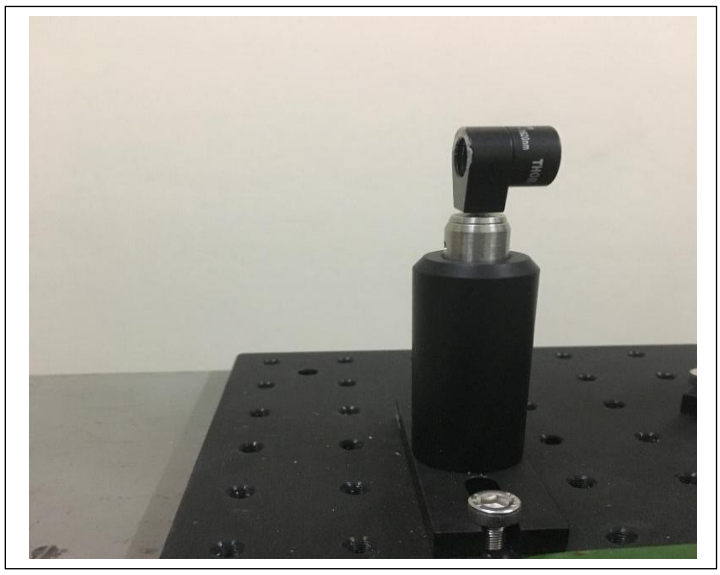

Figure (2.5): Convex Lens

2.2.3 Spectrometer

A spectrometer model BLUE-Wave LSR-uv2-14(manufactured by StellarNet Inc) are a fiber optically coupled instruments with selection of measurements in the wavelength range 200-400 nm, (as shown in figure (2.6)).The specifications of the spectrometer are listed in table (2.2).

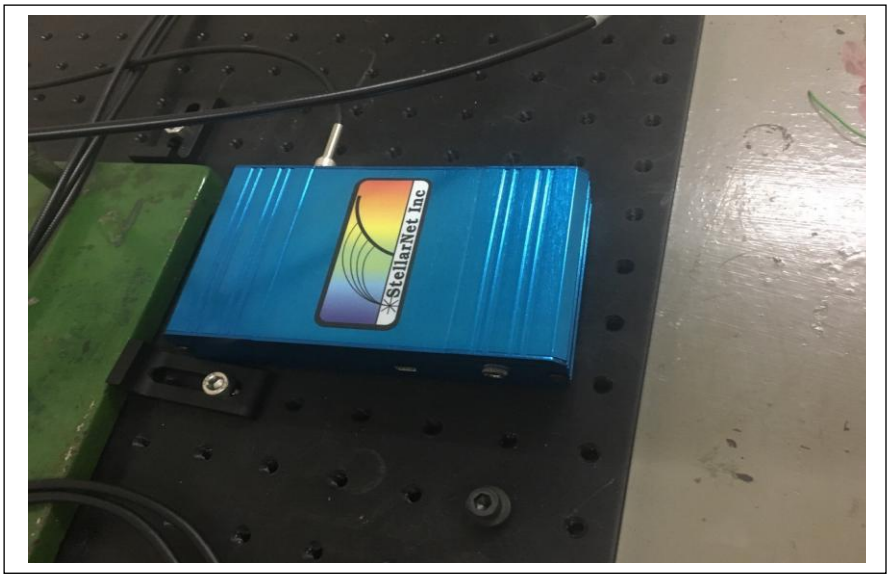

Figure (2.6): Spectrometer

Table (2.2): Specifications of spectrometer.

Specifications	
Model	BLUE-Wave LSR-uv2-14
Detector Type	CCD, 2k/3k pixels
Detector range	200-400 nm
Pixel size	14 x 200 µ m or 7 x 200 µ m
Weight	14 ounces
Operating systems	Windows and Linux2, Andriod2, iOS2

2.2.4 Monochromator

The monochromotor series of UV-VIS-NIR monochromators (model: MC1-01) is also used in this setup. This devise is manually operated that utilizes a dial for wavelength selection, and a four digit counter for wavelength readout, as shown in Figure (2.7), and specifications of monochromator are listed in table (2.3).

Figure (2.7): Monochromator.

Table (2.3): Specifications of monochromator.

Specifications	
Effective aperture	3.9
focal length	74mm
Grating	2 cm square
Slit	300μ× 4mm
Operating temperature	-20^{o} C to +80^{o} C
Wavelength accuracy	±0.2%

2.2.5 Energy Meter

Energy meter (model QE12LP-S-MB-INT-DO manufactured by gentec-eo) was used to measuring the energy of plasma emission line, as shown in Figure (2.8).

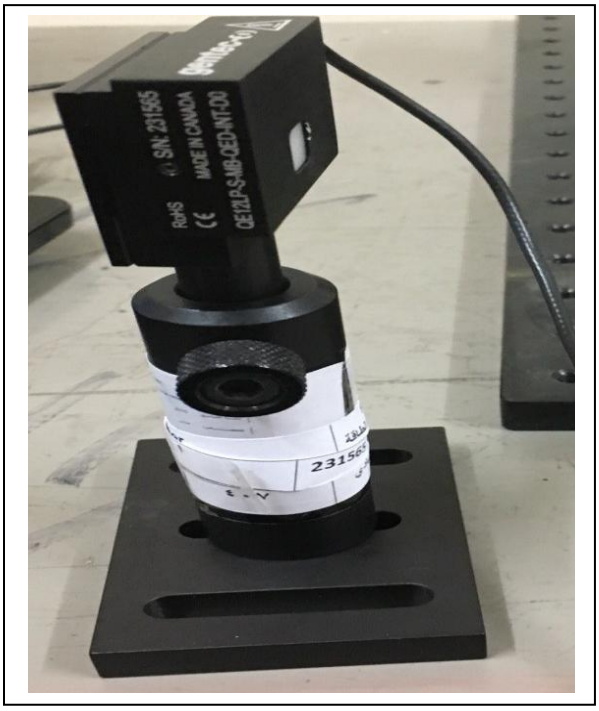

Figure (2.8): Energy meter

2.3 Holmium Rod

The material has been used in this work was a pure holmium rod, as shown in figure (2.9).

Figure (2.9): Holmium Rod

The atomic number of Holmium (Ho) was 67. It is eleventh rare Earth element, and called lanthanides, that has only one stable isotope (^{165}Ho) [81]. The properties of this holmium rod listed in table (2.4).

Table (2.4): The properties of the Holmium rod used in experimental work.

Specifications	
Symbol	Ho
Atomic Number	67
Chemical Properties	99.9% (REO basis)
Element Category	Rare Earth Metal
Phase at STP	Solid
Atomic Mass [amu]	164.9303
Density at STP [g/cm3]	8.795
Electron Configuration	4f11 6s2
Possible Oxidation States	+3
1st Ionization Energy [eV]	6.0216
Year of Discovery	1879

2.4 The Cowan Code:

The Cowan code is the most widely available numerical computer code for calculating atomic structure. This FORTRAN code was comprised by Robert D. Cowan in 1968 [82]. The Cowan code calculates the wavelength, λ, and weighted oscillator strength, *gf* (a dimensionless quantity to express the strength of the transition), for a transition between two states. The theoretical transitions are then convolved with a broadening function or an instrument function to match experimental results [83].

ChapterThree

Results and Discussion

3.1Introduction

This chapter includes the results of the experimental and theoretical measurements of plasma emission characteristics which can be classified into two parts:

1- Optical emission spectroscopy (OES) technique. It studies the influences of the laser energy and pulse repetition rate on the emission lines of the laser induced plasma spectrum in air.

In this technique, a focused Q-switched Nd:YAG laser pulse on the surface of the holmium target is used to measure the emission spectra in the range of (200-400) nm.

2- Using Cowan code to get the emission spectra for different transitions of the holmium target.

The laser intensities used in this work with different laser energy, are listed in table (3.1).

Table (3.1): listed the laser intensities with different laser energy

Plus laser energy (mJ)	laser intensities ($W.cm^{-2}$)
600	6.18×10^{8}
650	6.69×10^{8}
700	7.21×10^{8}
750	7.72×10^{8}
800	8.24×10^{8}

3.2 Results

Different laser parameter had been used in this work. Different laser pulse energies of (600 mJ, 650 mJ, 700 mJ, 750 mJ, and 800 mJ) are focused each time with different repetition rate (1Hz, 5Hz, 10Hz, and 20Hz).

Four groups of laser parameters were used to get the result of the emission spectra of holmium at wavelength (200-400) nm.

3.2.1 Holmium Emission at 1Hz Repetition Rate

The first group of laser parameters that used different laser pulse energy of (600,650,700,750 and 800) mJ at fixed repetition rate (1Hz).

The maximum intensity of holmium line emission was at(ג = 345.75 nm) when the laser pulse energy is (600 mJ) with a maximum intensity of (40000), as shown in figure (3.1).

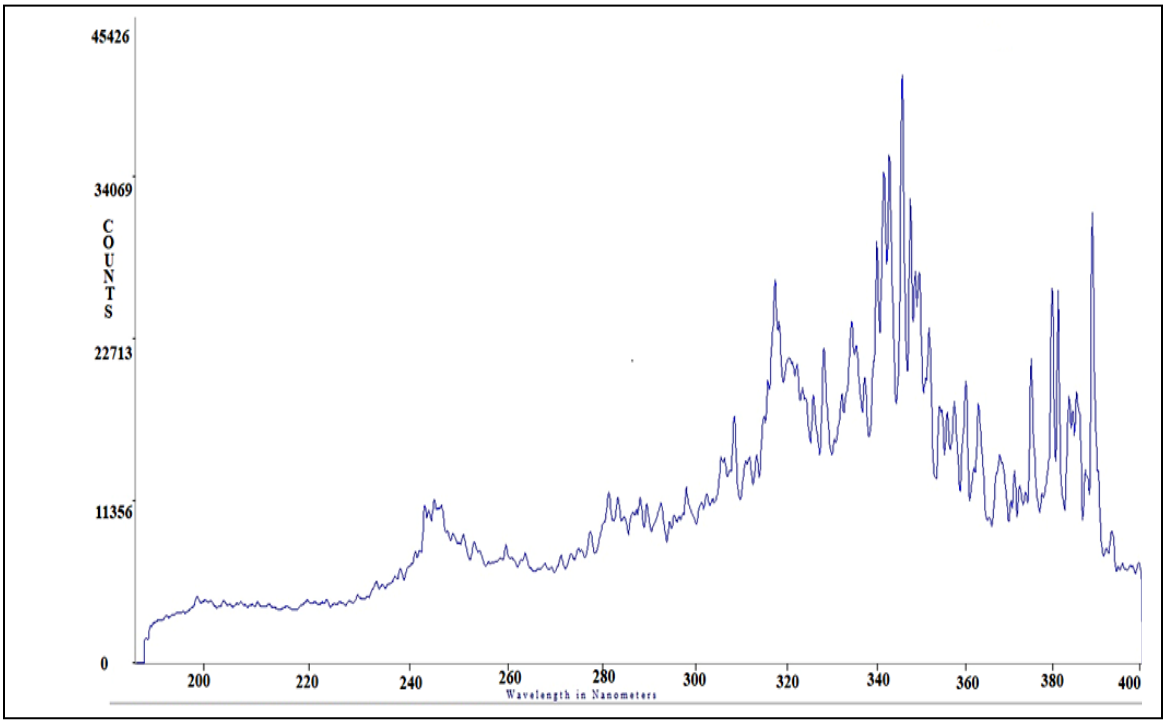

Figure (3.1): Emission spectra of 600 mJ laser energy at (1Hz) repetition rate

Figure (3.2) shows the emission spectra result when the laser pulse energy is (650 mJ). The result obtained from these parameter shows many emission line spectra of holmium , and the strongest one is (345.75 nm) with a maximum intensity of (59000).

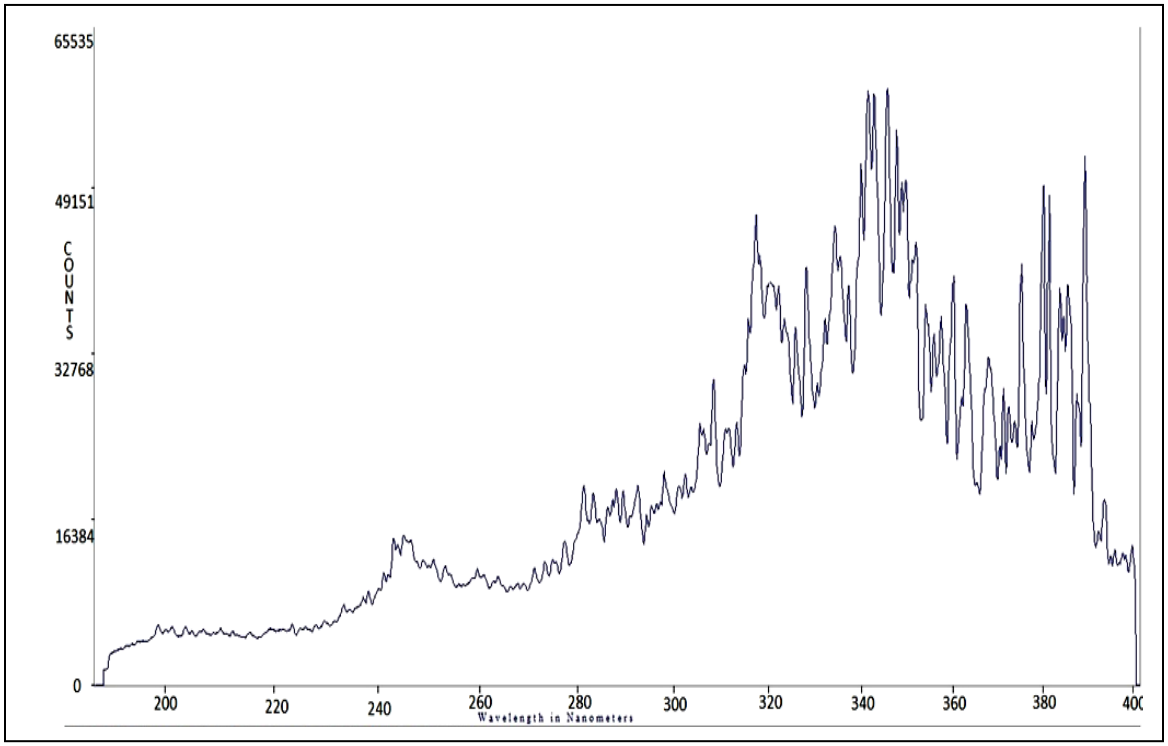

Figure (3.2): Emission spectra of 650 mJ laser energy at (1Hz) repetition rate

When the laser energy was increased to (700 mJ), the intensity of the emission line is also increased, and the maximum intensity of emission spectra was (65535 at ג = 341.43 nm), as shown in the figure (3.3).

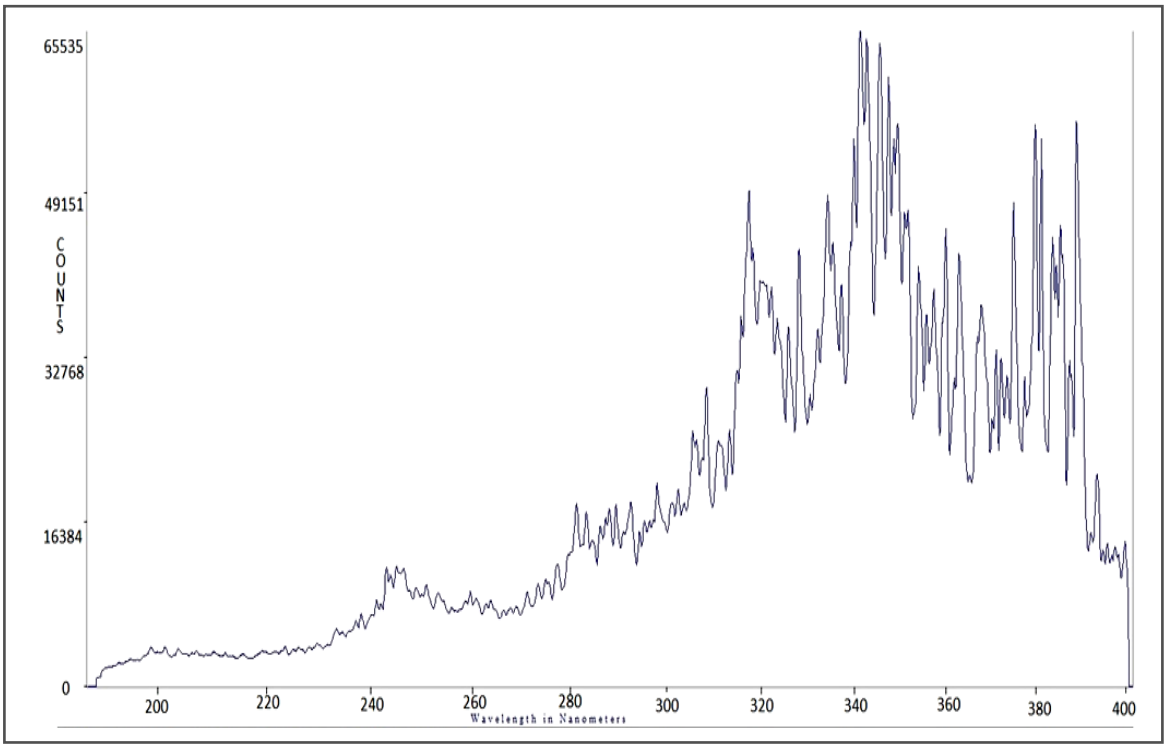

Figure (3.3): Emission spectra of 700 mJ laser energy at (1Hz) repetition rate

If the laser pulse energy is increased to (750 mJ), the intensity of the emission line is also increased, and the maximum intensity of emission spectra was (70000 at ג = 341.54 nm), as shown in the figure (3.4)

The results of figure (3.5) indicate that, when the laser pulse energy is increased to (800 mJ), the maximum intensity of the emission spectra was (80000 at ג = 341.54 nm) .

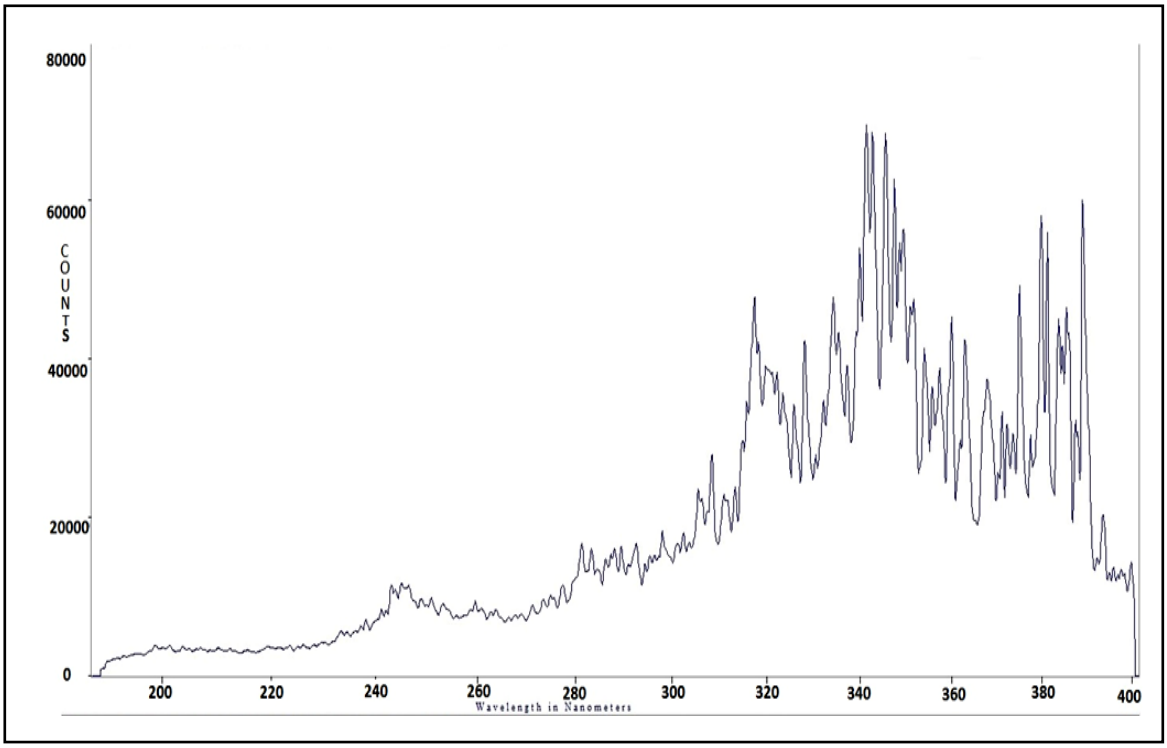

Figure (3.4): Emission spectra of 750 mJ laser energy at (1Hz) repetition rate

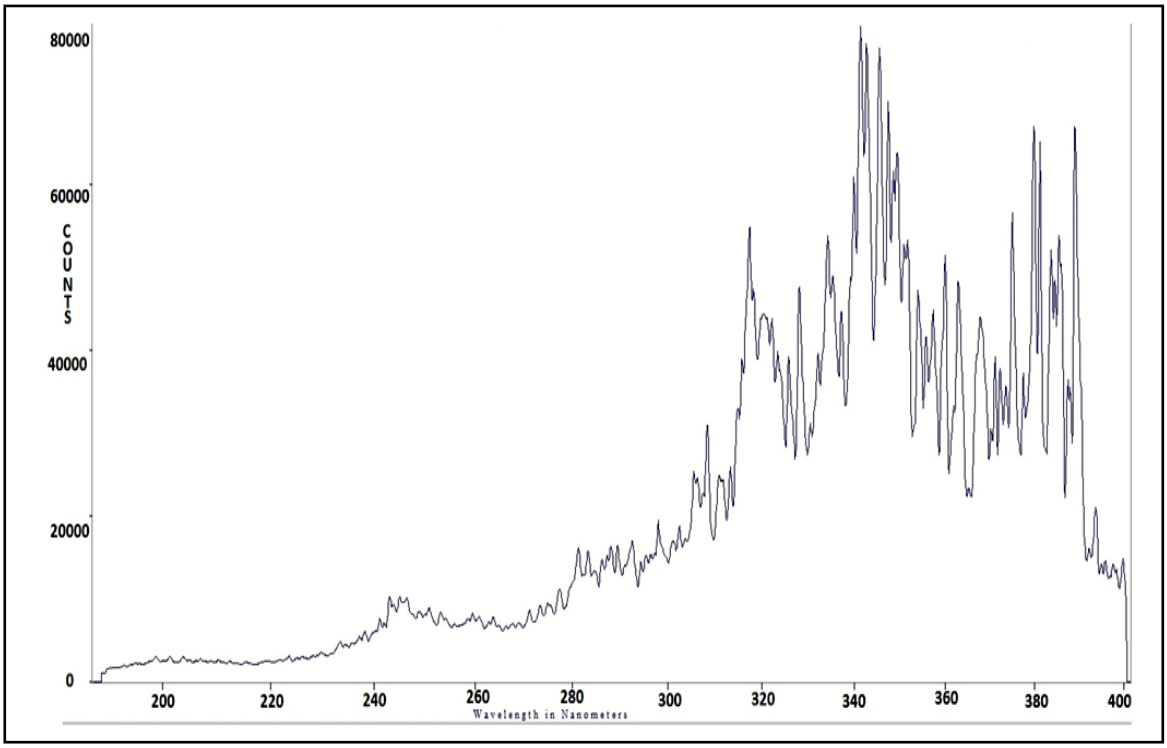

Figure (3.5): Emission spectra of 800 mJ laser energy at (1Hz) repetition rate

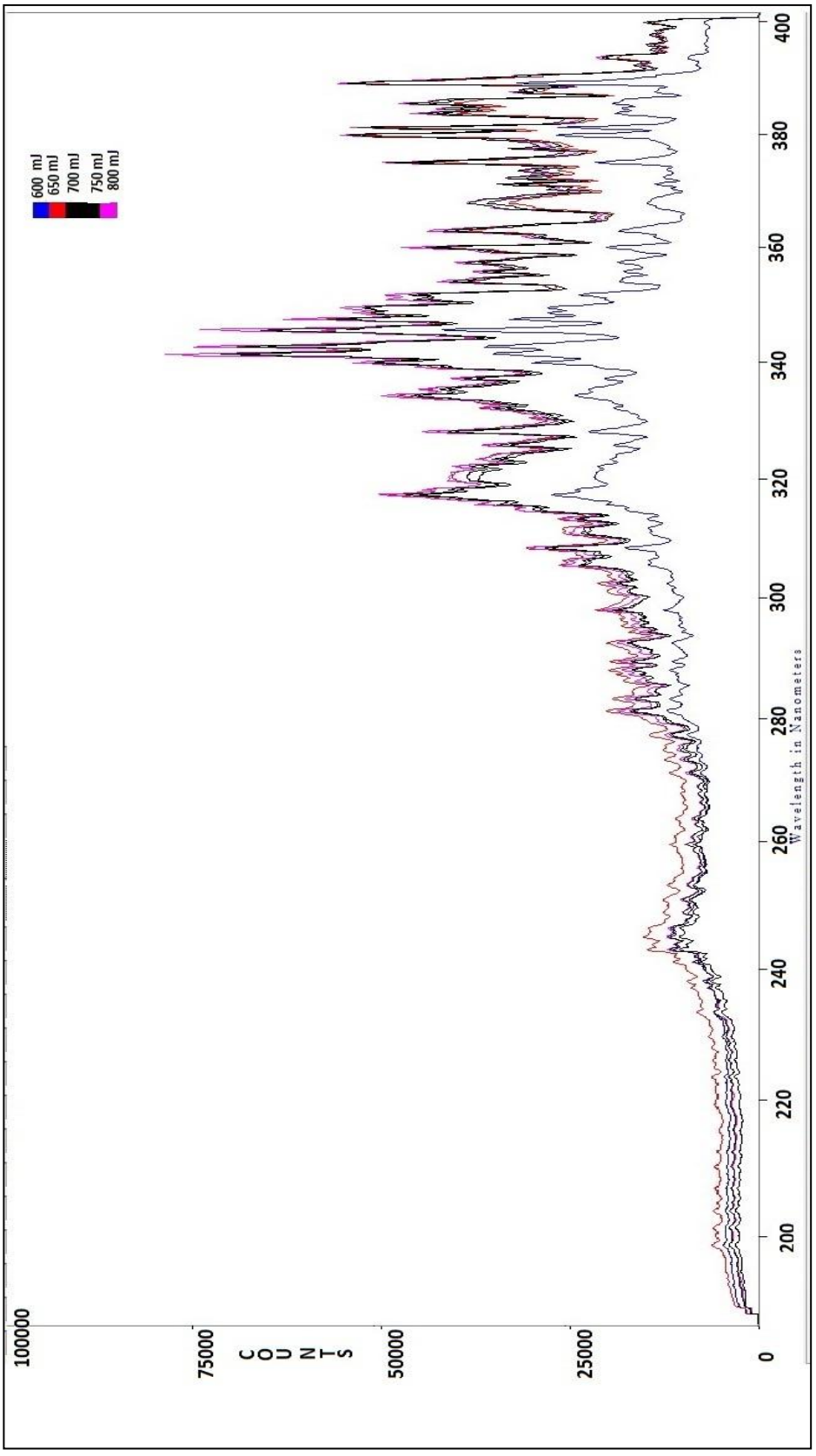

Figure (3.6): Emission spectra of laser induced holmium plasma with different laser energies at (1Hz) repetition rate

Figure (3.6) represents all the results for different laser pulse energies used in this work. The maximum holmium line emission intensity was 80000 at 341.54 nm , when used laser pulse energy 800 mJ .

3.2.2 Holmium Emission at 5Hz Repetition Rate

The second group with different laser energies of (600,650,700,750 and 800) mJ at fixed repetition rate 5hz ,had been used to get the result of the emission spectra of holmium at wavelength (200-400) nm .

The maximum intensity of holmium line emission at (ג = 345.75 nm), when the laser pulse energy is (600 mJ) was (58000) , as shown in figure (3.7).

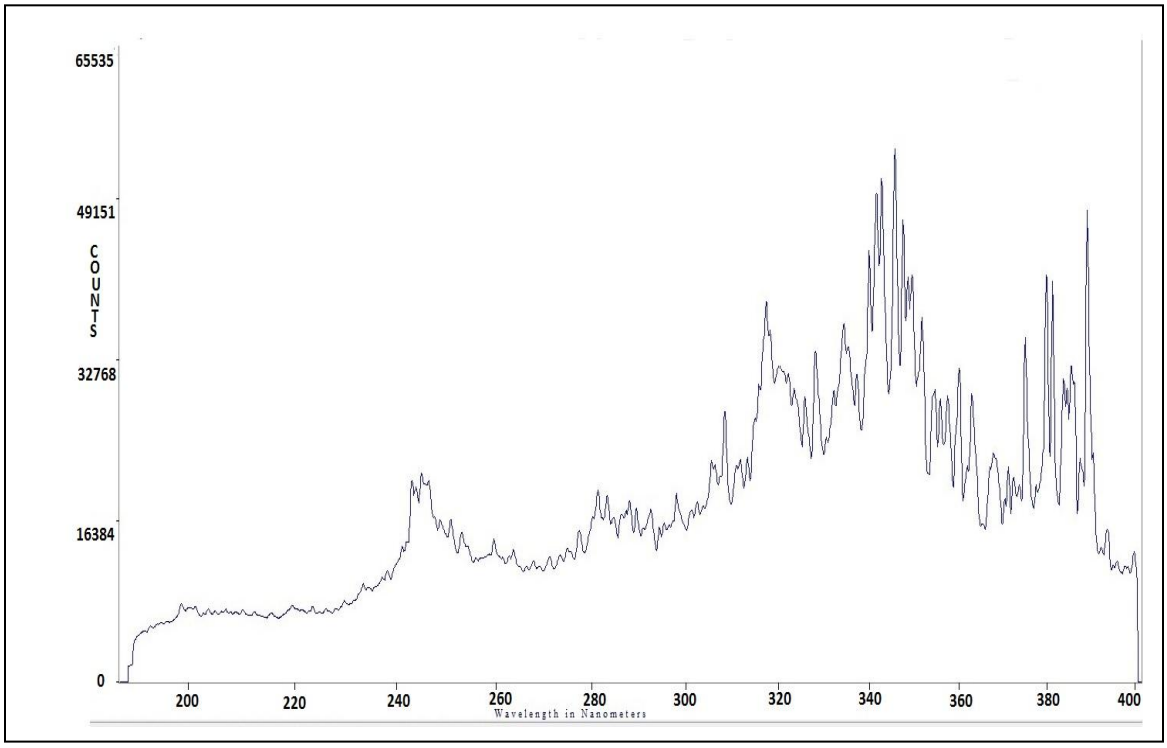

Figure (3.7): Emission spectra of 600 mJ laser energy at (5Hz) repetition rate

Figure (3.8) shows the emission spectra result when the laser pulse energy is 650 mJ. The result obtained from these parameter shows many line emission spectra of holmium , and the strongest one is (345.75 nm) with a maximum intensity of (62535).

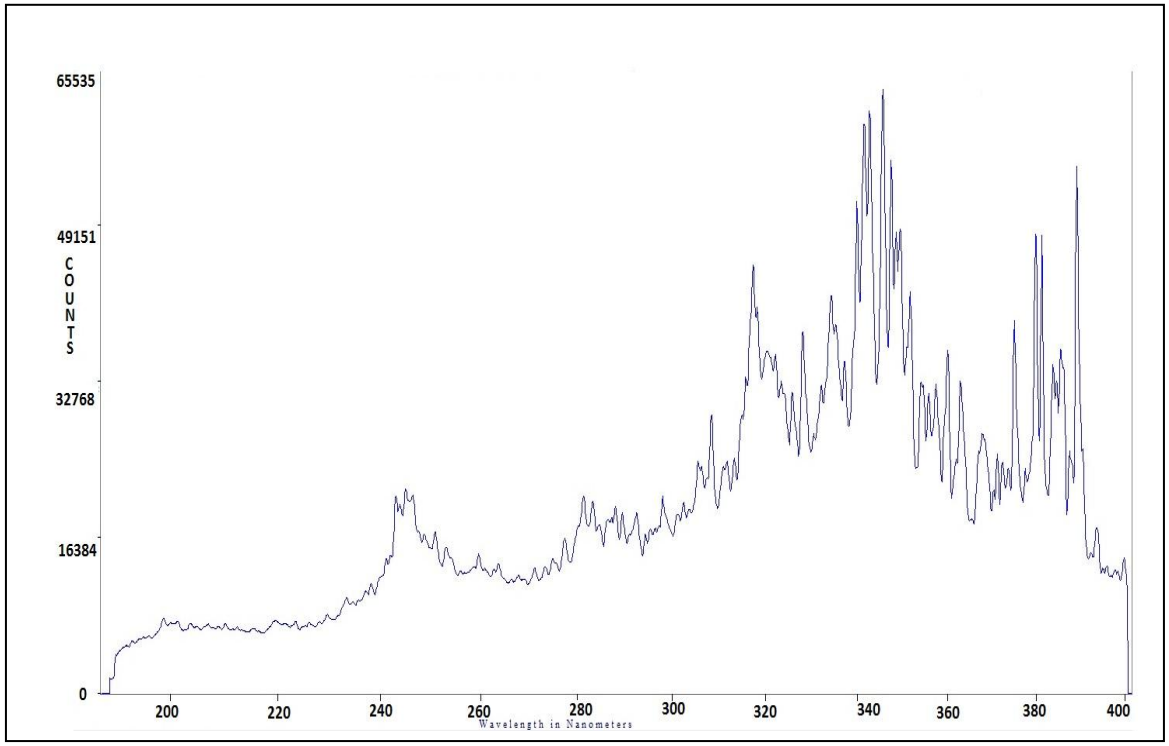

Figure (3.8): Emission spectra of 650 mJ laser energy at (5Hz) repetition rate

When the laser energy was increased to 700 mJ, the intensity of the emission line is also increased, and the maximum intensity of emission spectra was 70000 at 345.75 nm, as shown in the figure (3.9).

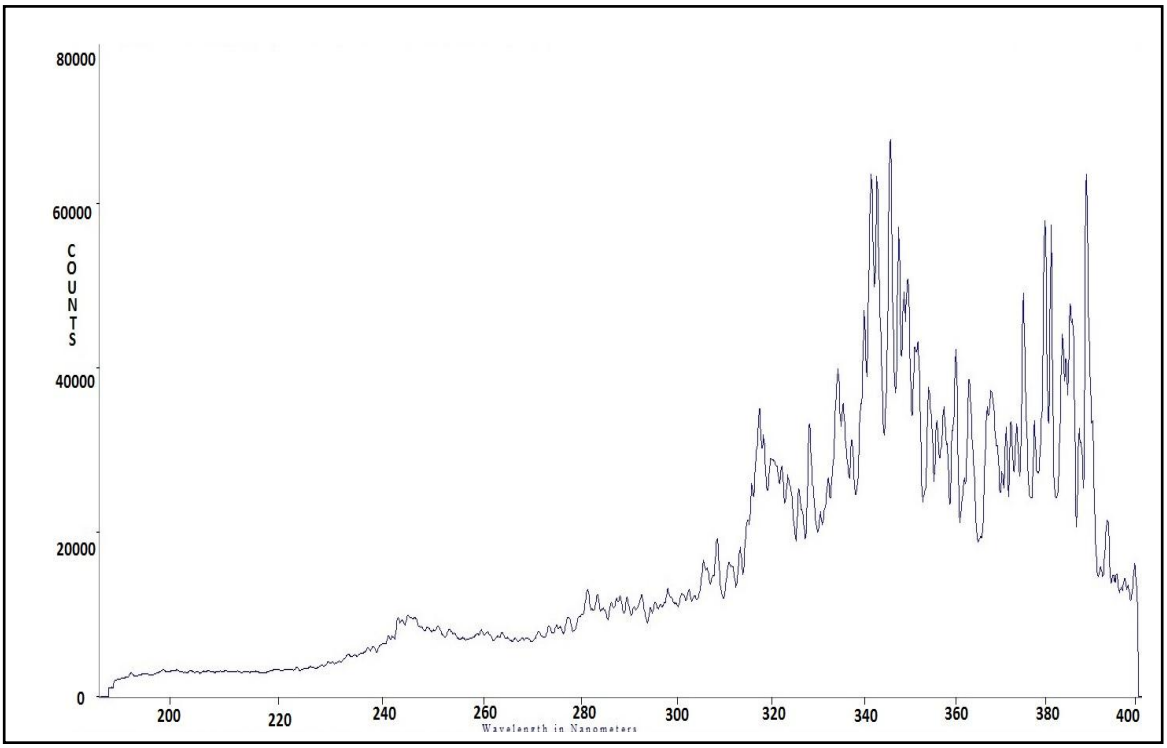

Figure (3.9): Emission spectra of 700 mJ laser energy at (5Hz) repetition rate

When the laser pulse energy is (750 mJ), the maximum emission spectra intensity was appeared at (341.54 nm, 342.76 nm and 345.53 nm) respectively, and the maximum line emission intensity was (75000) , as shown in figure (3.10).

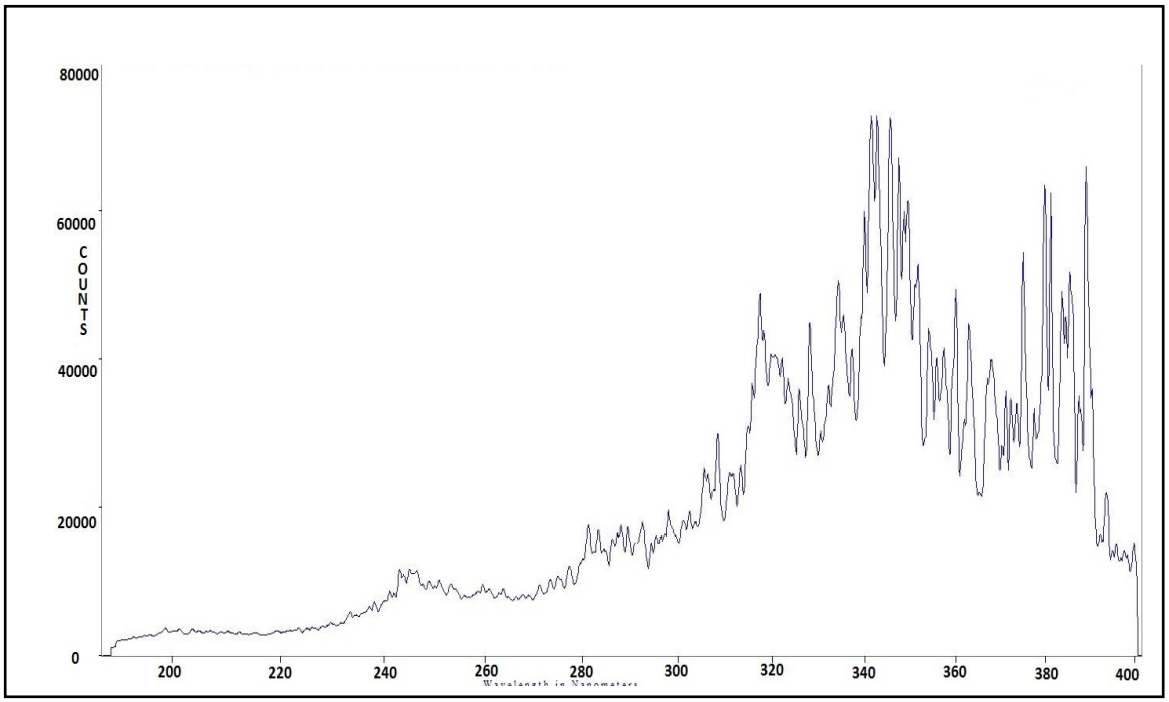

Figure (3.10): Emission spectra of 750 mJ laser energy at (5Hz)repetition rate

The results of figure (3.11) indicate that, when the laser pulse energy is increased to (800 mJ), the maximum intensity of emission spectra was 80000 at 345.75 nm .

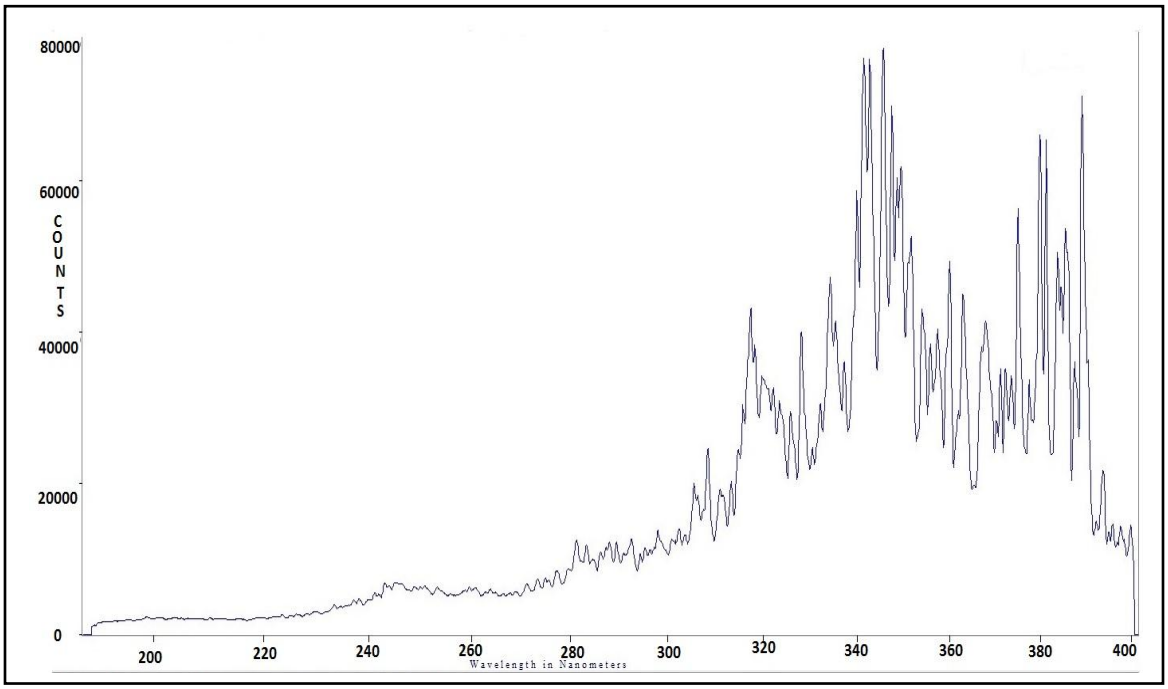

Figure (3.11): Emission spectra of 800 mJ laser energy at (5Hz)repetition rate

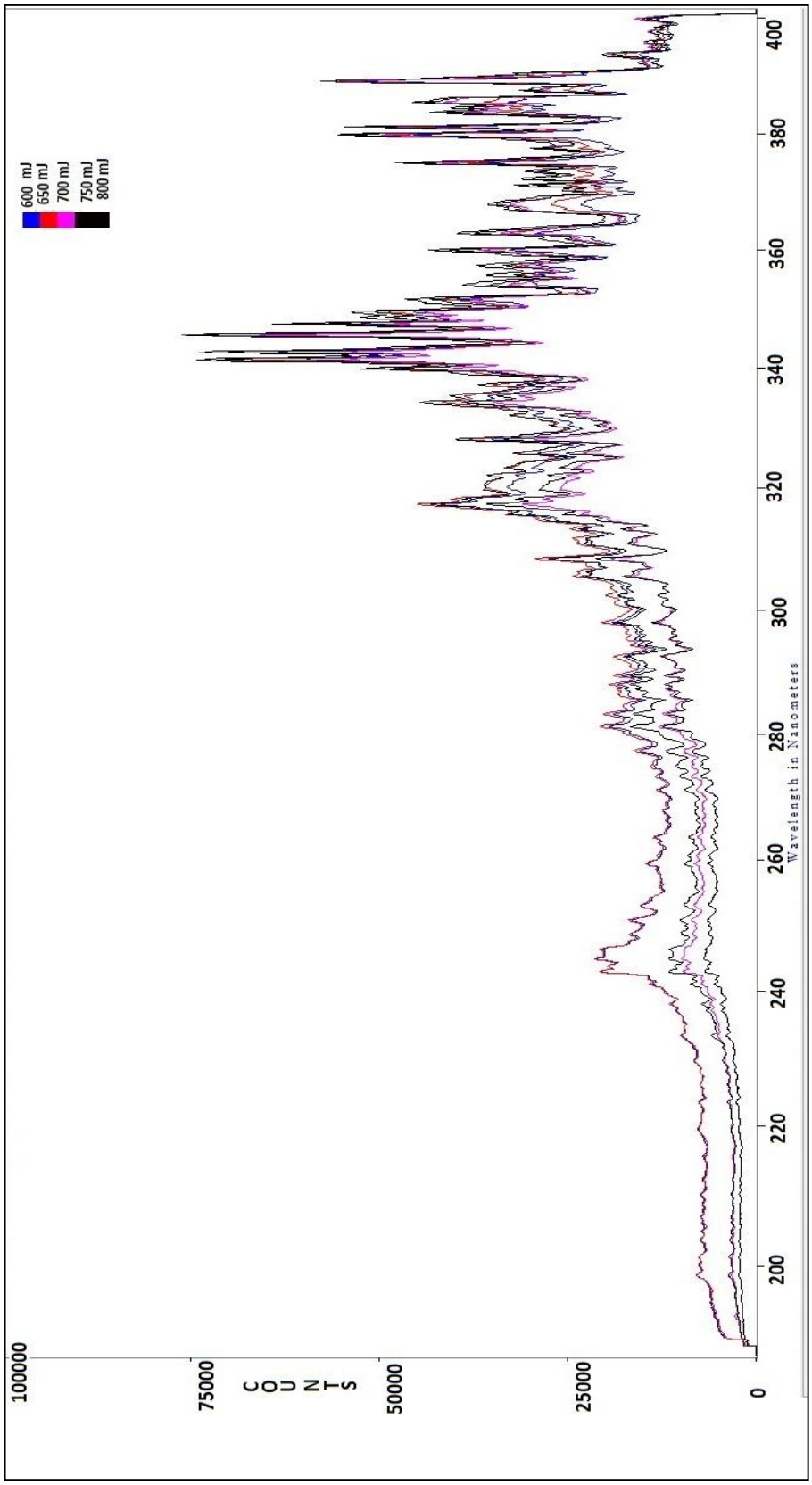

Figure (3.12): Emission spectra of laser induced holmium plasma with different laser energies at (5Hz) repetition rate

Figure (3.12) indicate that the maximum intensity of holmium line emission appeared at (345.75 nm), when the laser energies are (600 mJ, 650 mJ, 700 mJ, and 800 mJ) respectively . The maximum intensity was (80000).

3.2.3 Holmium Emission at 10Hz Repetition Rate

The third group of different laser energies of (600,650,700,750 and 800) mJ at 10 Hz repetition rate had been used.

When the laser pulse energy was (600 mJ) , the maximum intensity of holmium line emission was 40000 at (λ = 345.75 nm), as shown in figure (3.13) .

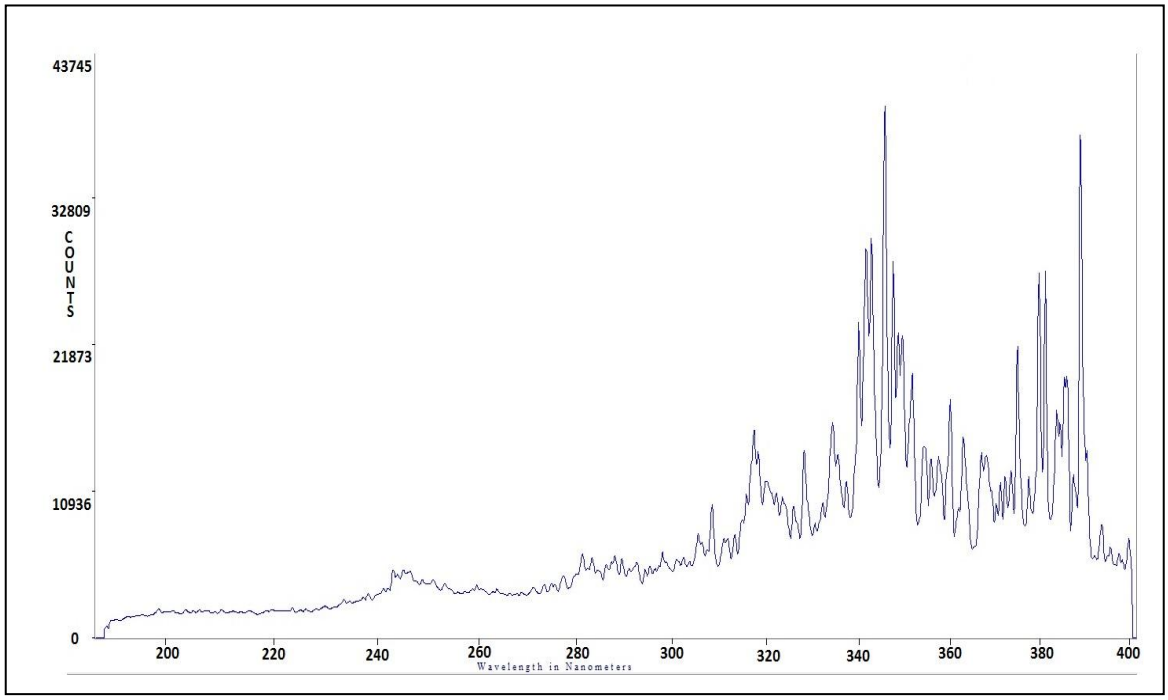

Figure (3.13): Emission spectra of 600 mJ laser energy at (10Hz) repetition rate

Figure (3.14) shows the emission spectra result when the laser pulse energy is (650 mJ). The result obtained from these parameters shows many line emission spectra of holmium, and the strongest one is (345.53 nm) with a maximum intensity of (45000).

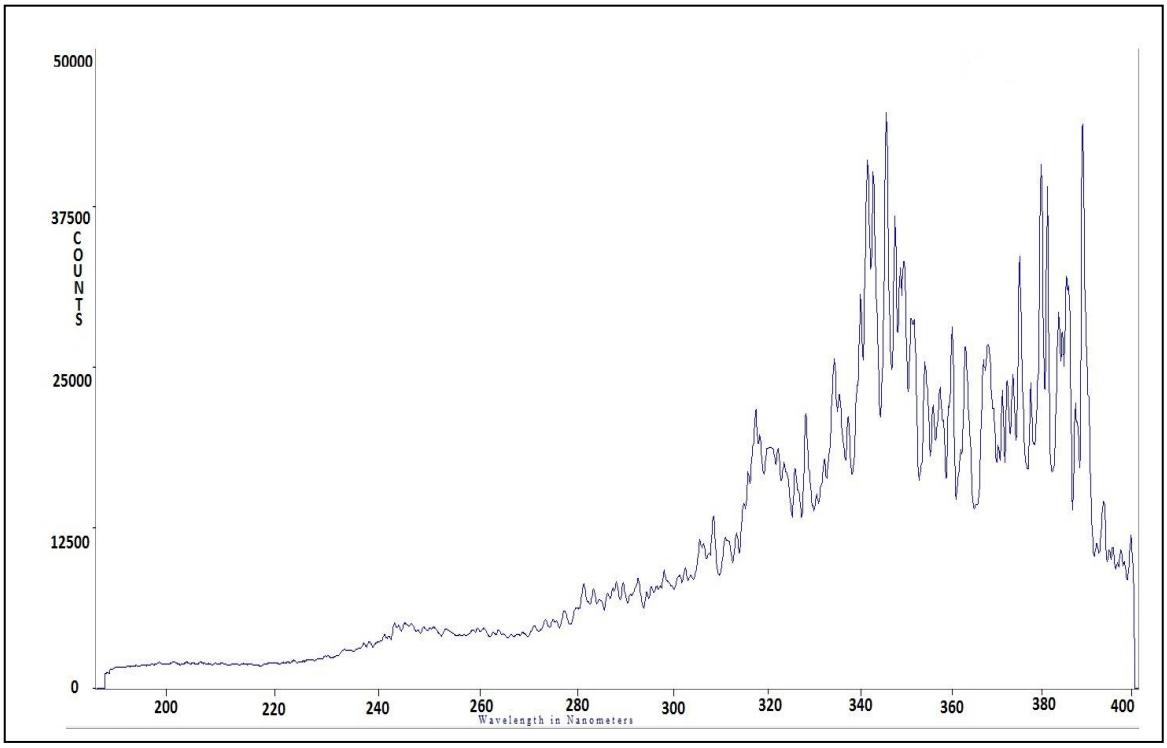

Figure (3.14): Emission spectra of 650 mJ laser energy at (10Hz) repetition rate

When the laser energy was increased to (700 mJ), the intensity of the emission line is also increased, and the maximum intensity of emission spectra was (51070 at ג = 345. 53 nm), as shown in the figure (3.15).

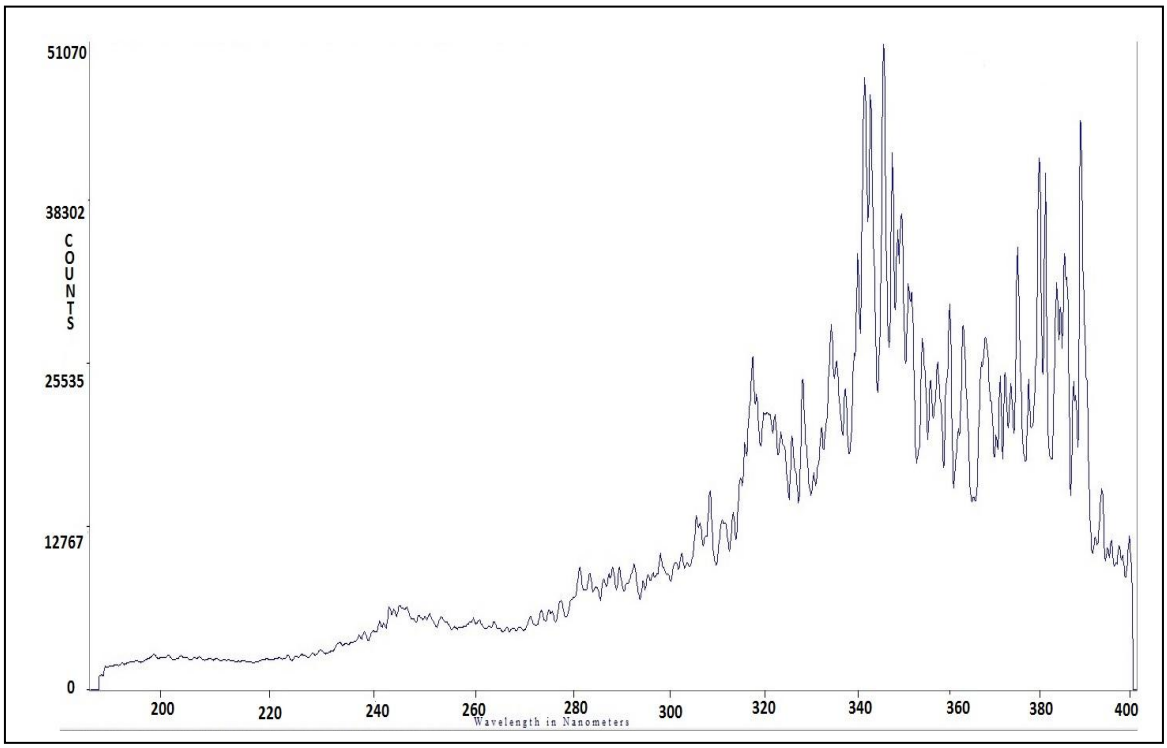

Figure (3.15): Emission spectra of 700 mJ laser energy at (10Hz) repetition rate

The maximum intensity, obtained from laser pulse energy of 750 mJ was 65000 appeared at 345.53 nm, as shown in figure (3.16)

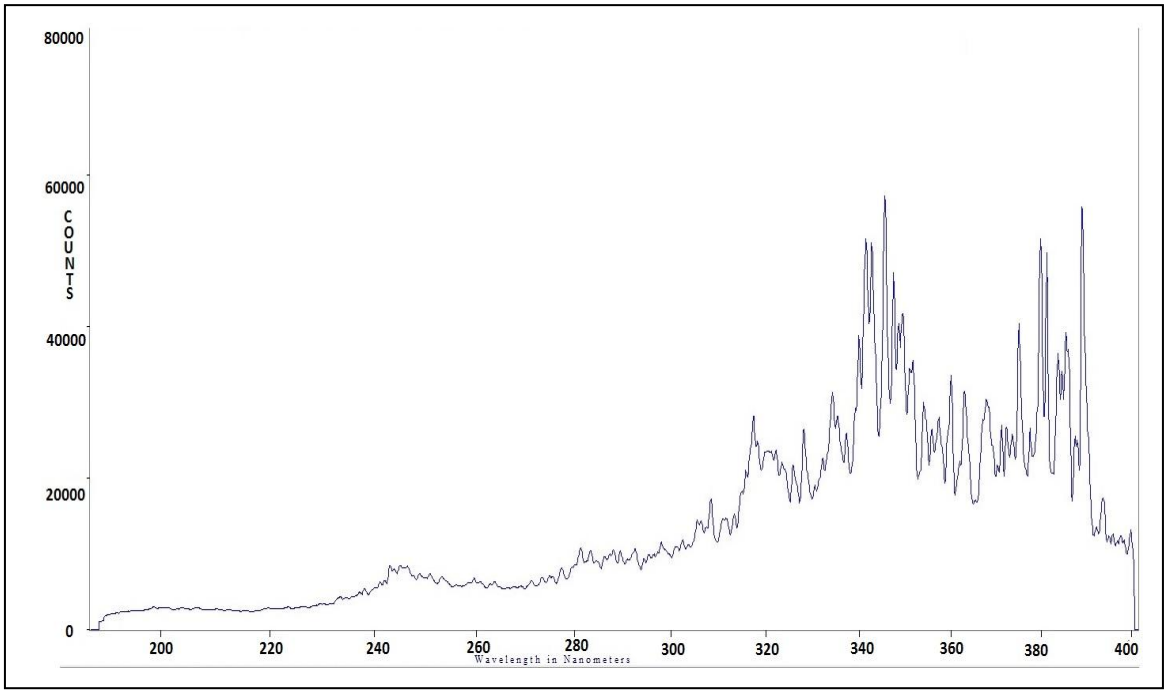

Figure (3.16): Emission spectra of 750 mJ laser energy at (10Hz) repetition rate

The results of figure (3.17) explain that, when the laser pulse energy is increased to 800 mJ, the maximum intensity of the holmium line emission spectra was 77000 at 345.64nm.

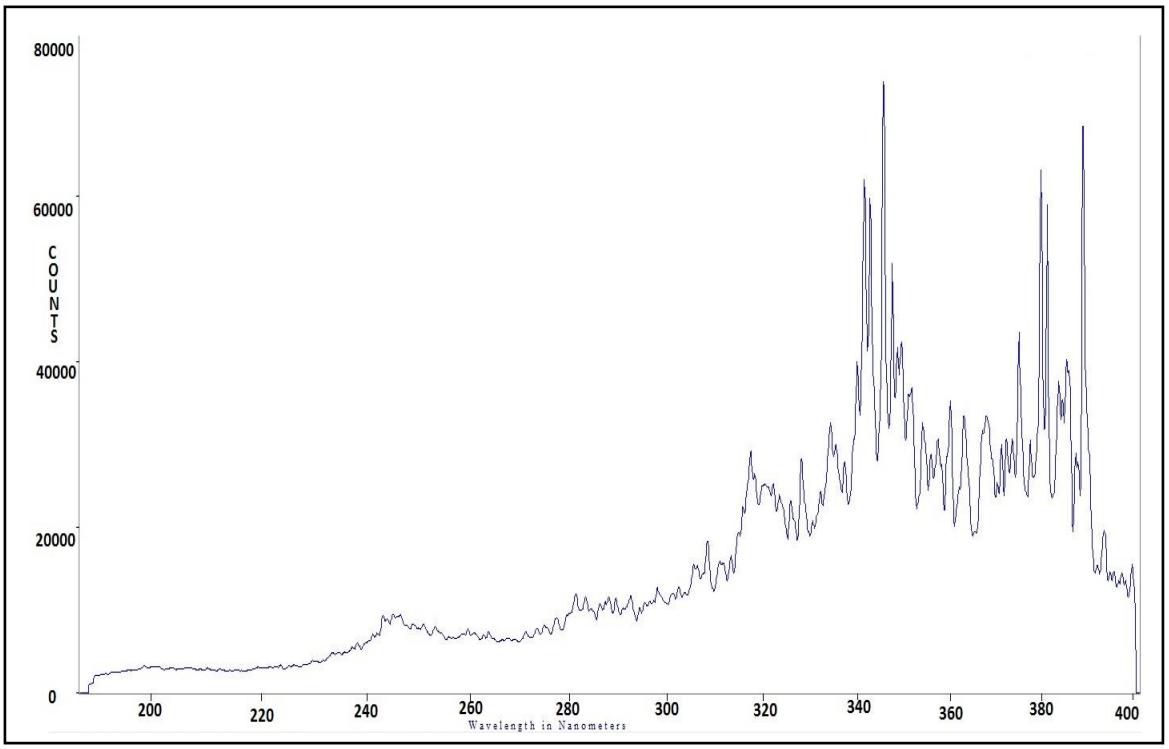

Figure (3.17): Emission spectra of 800 mJ laser energy at (10Hz) repetition rate

Figure (3.18), shows all the result obtained for different laser parameters at 10Hz repetition rate

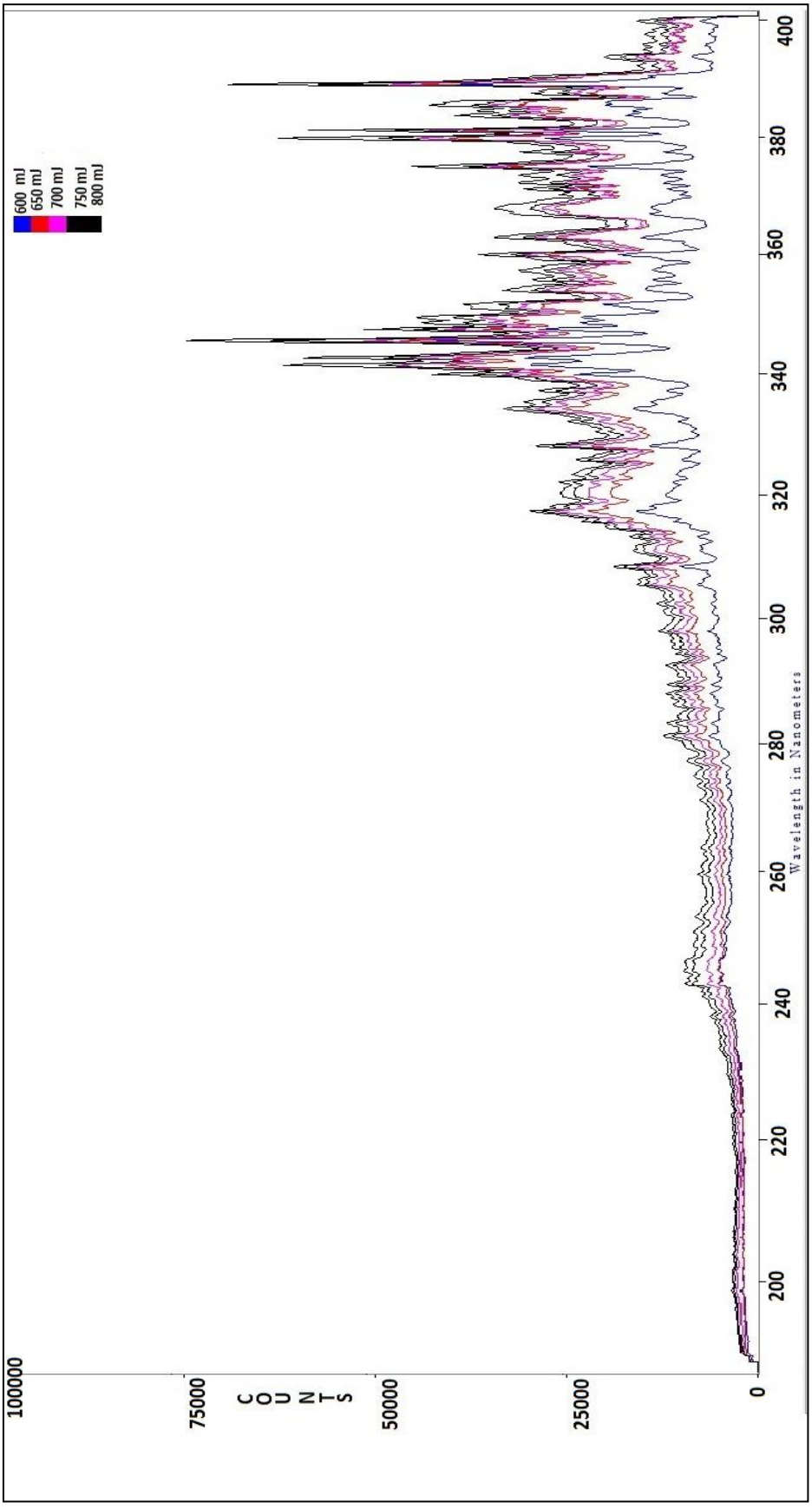

Figure (3.18): Emission spectra of laser induced holmium plasma with different laser energies and (10Hz) repetition rate

3.2.4 Holmium Emission at 20 Hz Repetition Rate

The fourth group with different laser energies of (600,650,700,750 and 800) mJ at 20 Hz repetition rate had been used to get the result of the emission spectra of holmium at wavelength (200-400) nm .

Using of (600mJ) laser pulse energy with repetition rate (20 Hz) leads to get a maximum holmium line emission intensity of 55000 at 345.53 nm. Fig. (3.19).

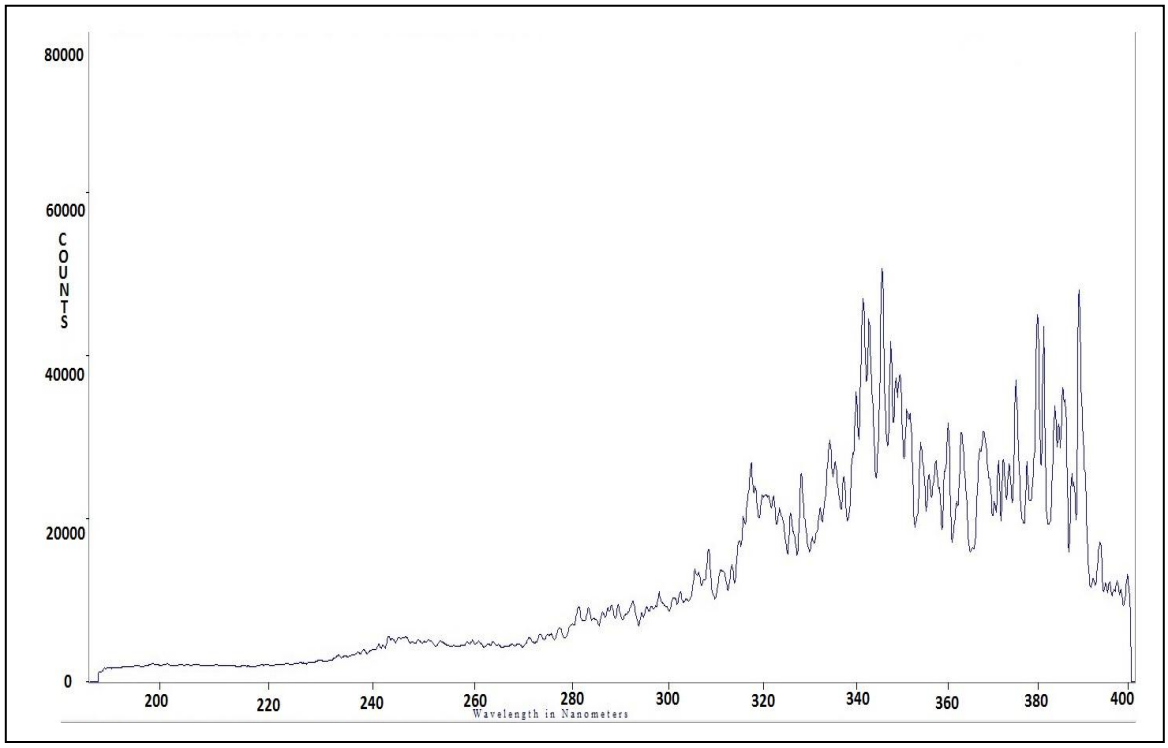

Figure (3.19): Emission spectra of 600 mJ laser energy with (20Hz) repetition rate

Figure (3.20) shows the emission spectra result when the laser pulse energy is (650 mJ).The result obtained from these parameter shows many line emission spectra of holmium ,and the strongest one is (341.43 nm) with a maximum intensity of (65535).

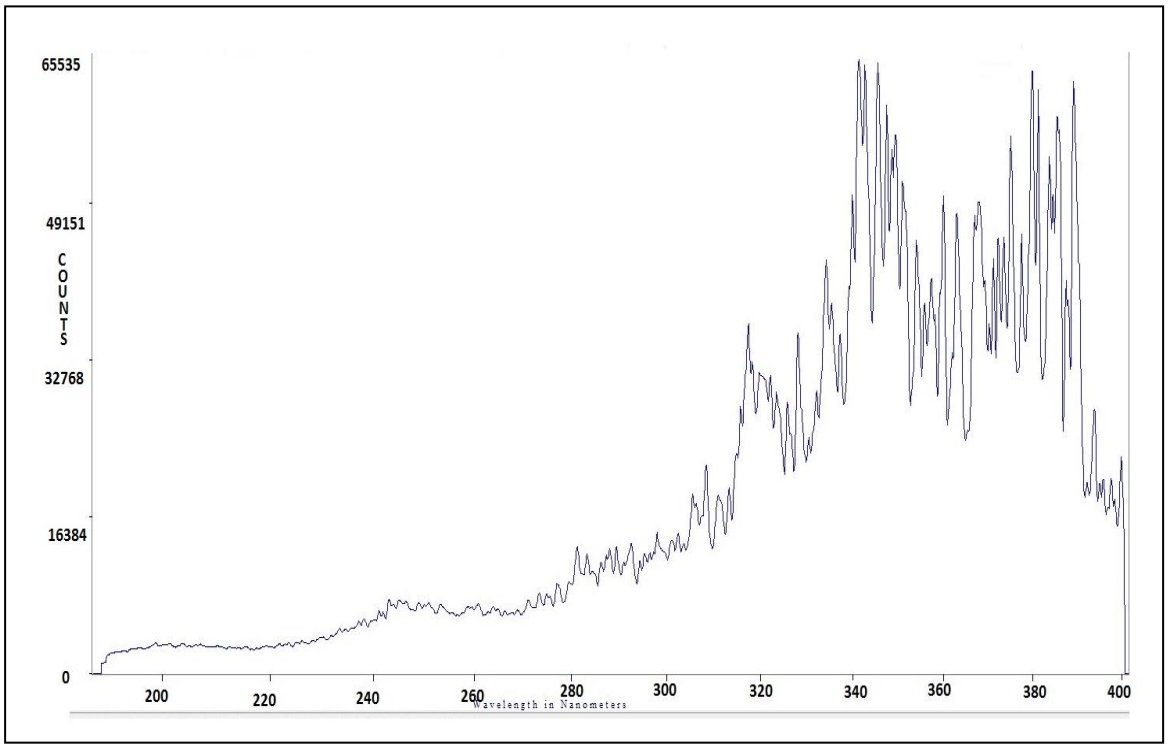

Figure (3.20): Emission spectra of 650 mJ laser energy at (20Hz) repetition rate

Increasing the laser pulse energy to (700 mJ) leads to increase the intensity of the emission line. Many line emission spectra have been observed. The maximum intensity was 70000 at 341.54 nm and 345. 53 nmrespectively, as shown in the figure (3.21).

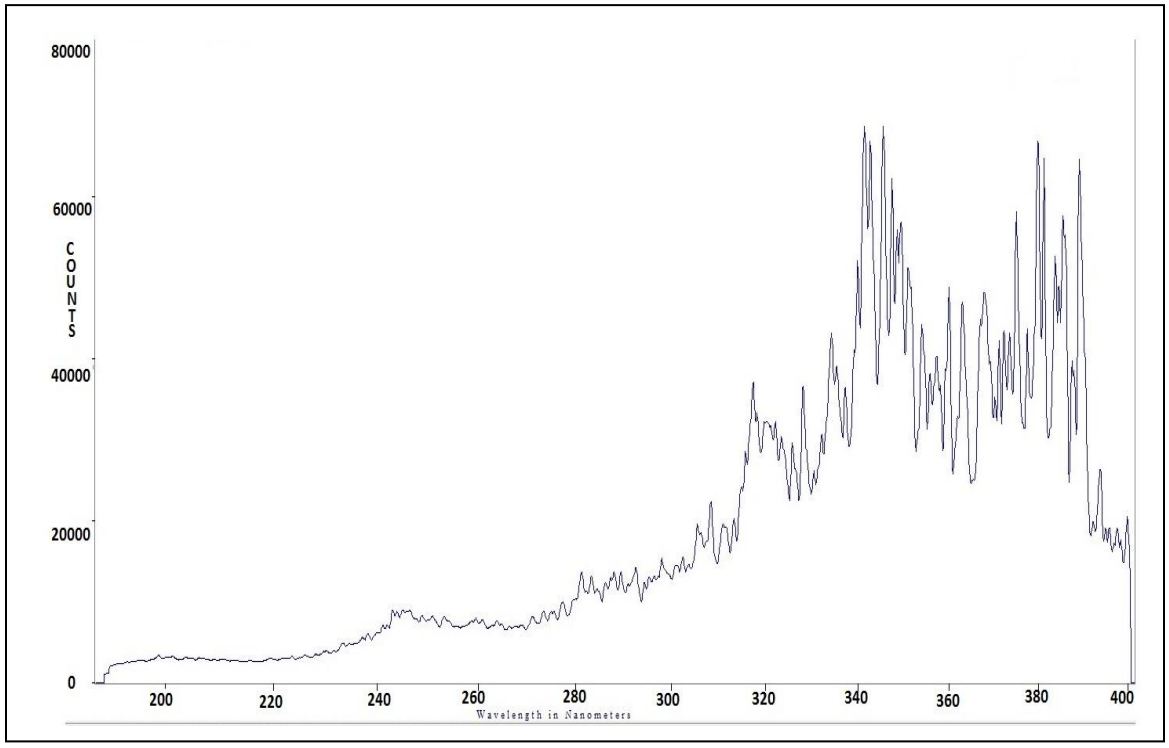

Figure (3. 21): Emission spectra of 700 mJ laser energy at (20Hz) repetition rate

When the laser pulse energy is (750 mJ), the maximum emission spectra intensity was 74000 at 341.54 nm and 345. 53 nm, respectively as shown in figure (3. 22).

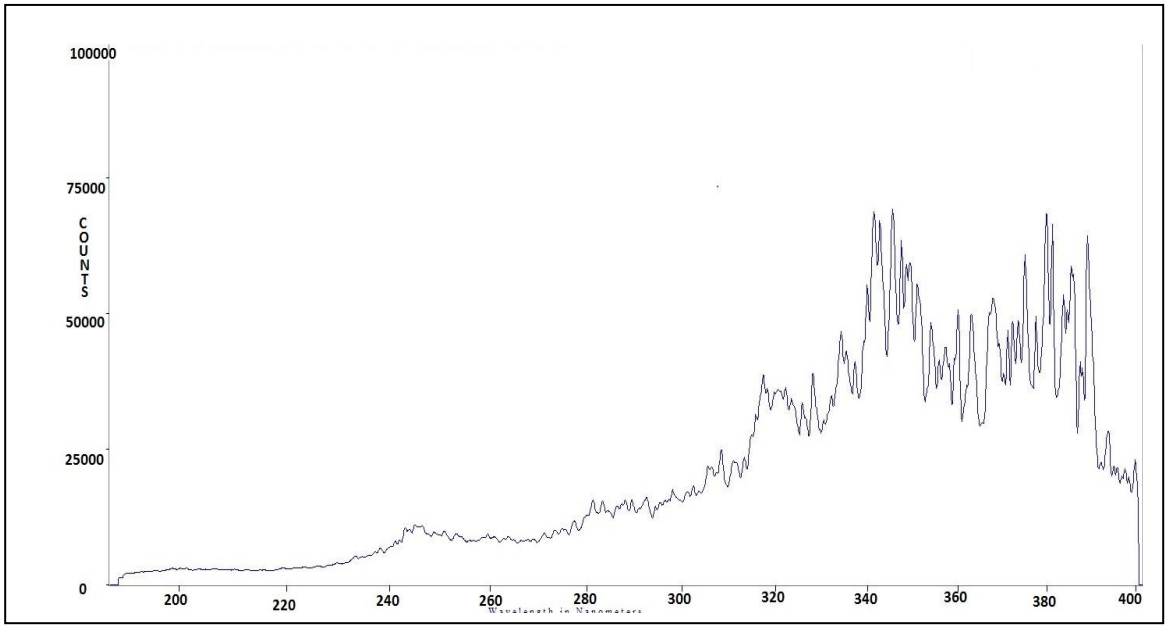

Figure (3.22): Emission spectra of 750 mJ laser energy with (20Hz) repetition rate

The results of figure (3.23) illustrated that, when the laser pulse energy increased to 800 mJ), the maximum intensity of emission spectra was 80000 at 341.54nm,342.76nm,and 345.53nm respectively.

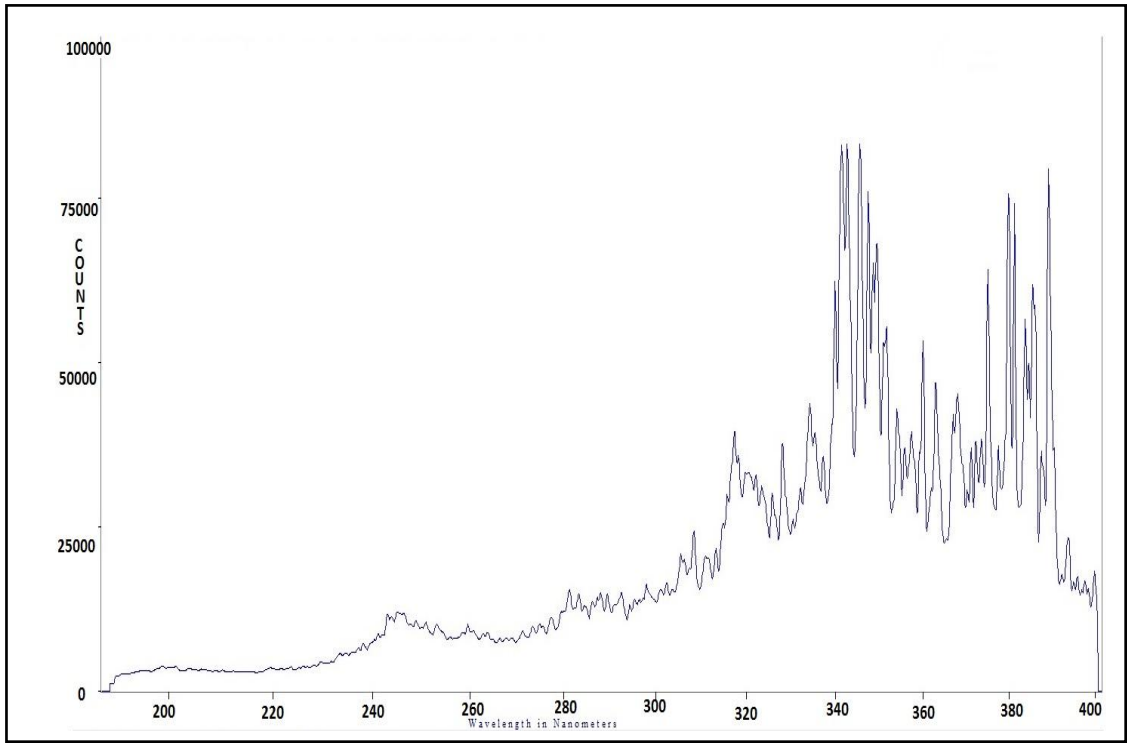

Figure (3. 23): Emission spectra of 800 mJ laser energy at (20Hz) repetition rate

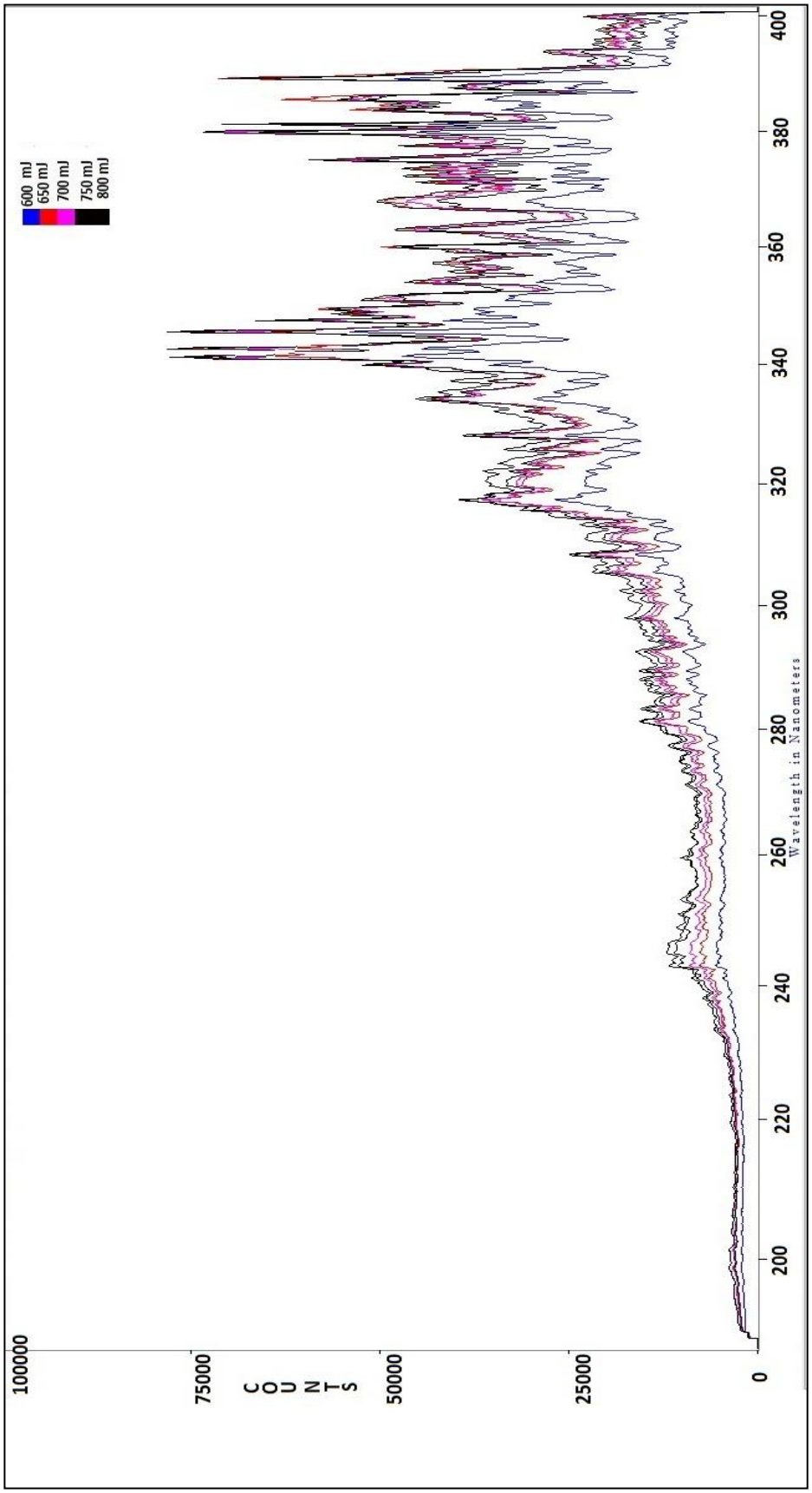

Figure (3.24): Emission spectra of laser induced holmium plasma with different laser energies and (10Hz) repetition rate

Figure (3.24) shows maximum line emission intensities appeared at 341.54nm, 342.76nm and 345.53nm with the maximum intensity at (80000), when the laser pulse energy is (800 mJ) and (20 Hz) repetition rate.

From the previous results, it can be seen that the intensities of the emission lines increase with increasing of the laser pulse energy and repetition rate. This results agreement with [84]. The increasing of the pulse energy means the increase of its absorption by the plasma leading to more ablation from the target and finally increasing of the emission line intensity, its agreement with [85].

The increase of laser power leads to increase ablation from the target which means more excited atoms and hence increasing in the height of the spectral line intensity, its agreement with [86].

3.2.5 Measurement of Individual Holmium Emission Line Intensity

To investigate the holmium emission spectra deeply, a new technique was used to measure each emission line with accuracy of (1nm). For this technique, a monochrometer was used to measure the intensity of each emission line. In this method the holmium emission spectra produced from a 650 mJ laser energy and 5Hz repetition rate. These parameters were chosed because the maximum emission line spectra are appeared.

The regain from (342-349) nm were covered by this technique because it implies the maximum emission line spectra with the emission line. Figures from ((3.25) to (3.32)) shows each emission line intensity for each nanometer.

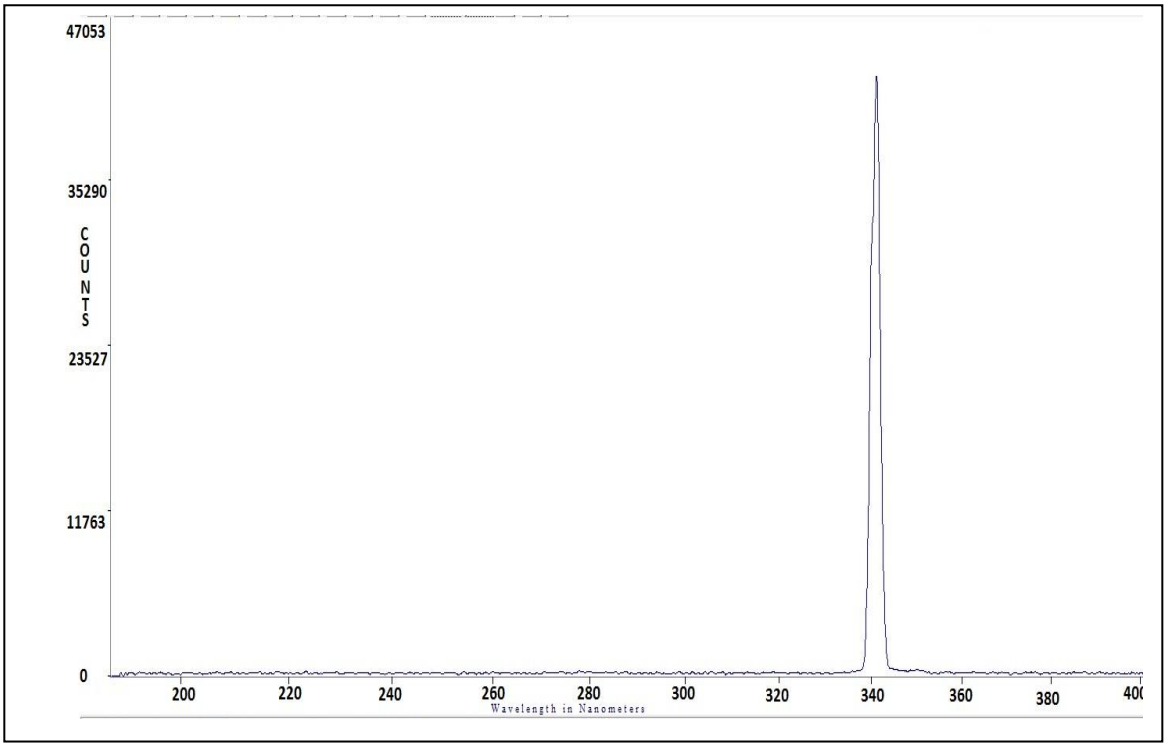

Figure (3.25): Emission line spectra at 342 nm

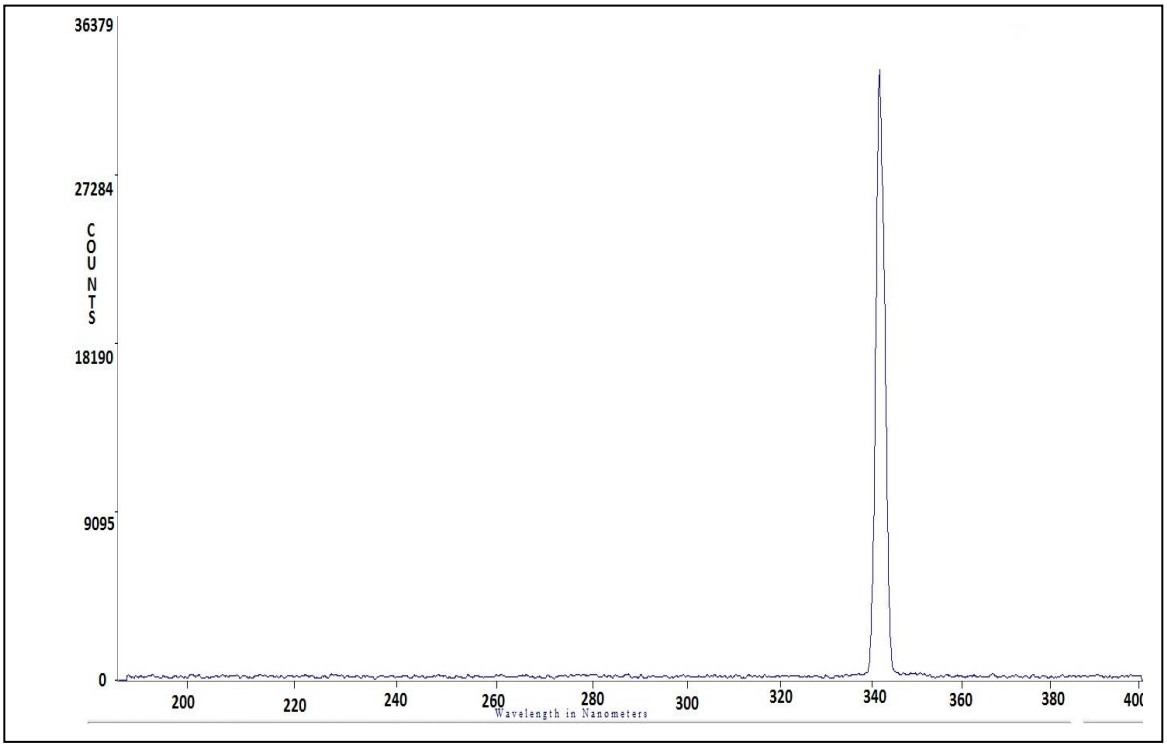

Figure (3.26): Emission line spectra at 343 nm

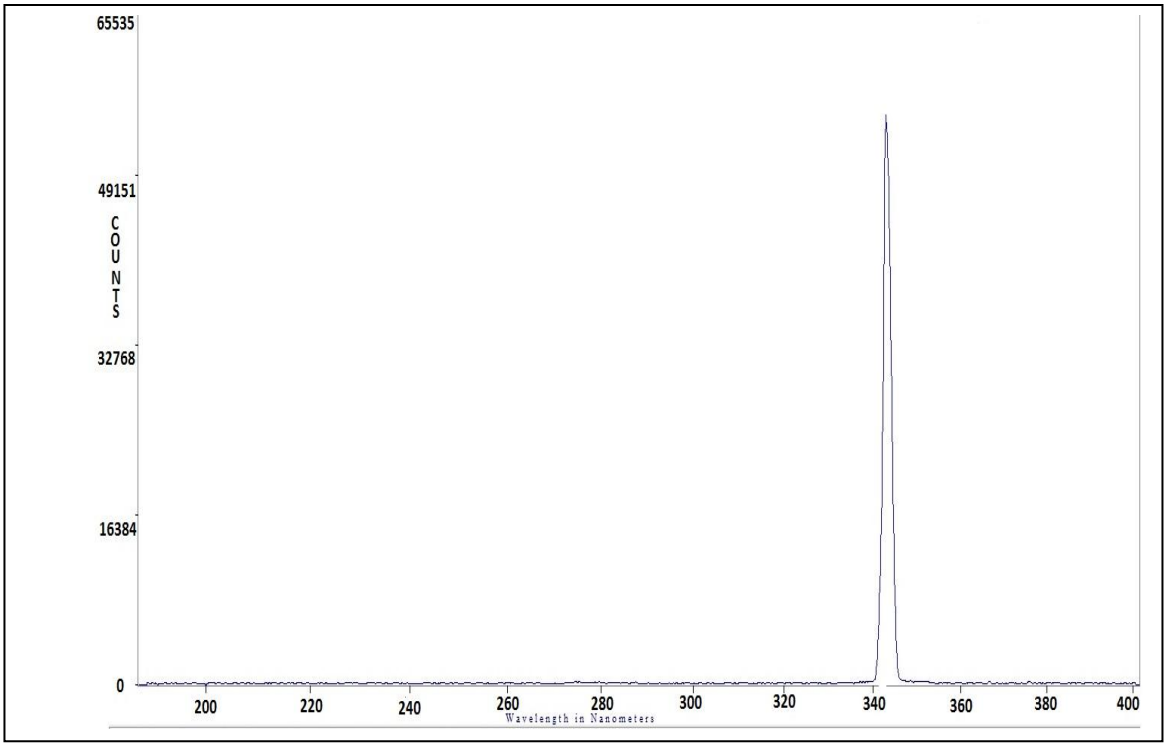

Figure (3.27): Emission line spectra at 344 nm

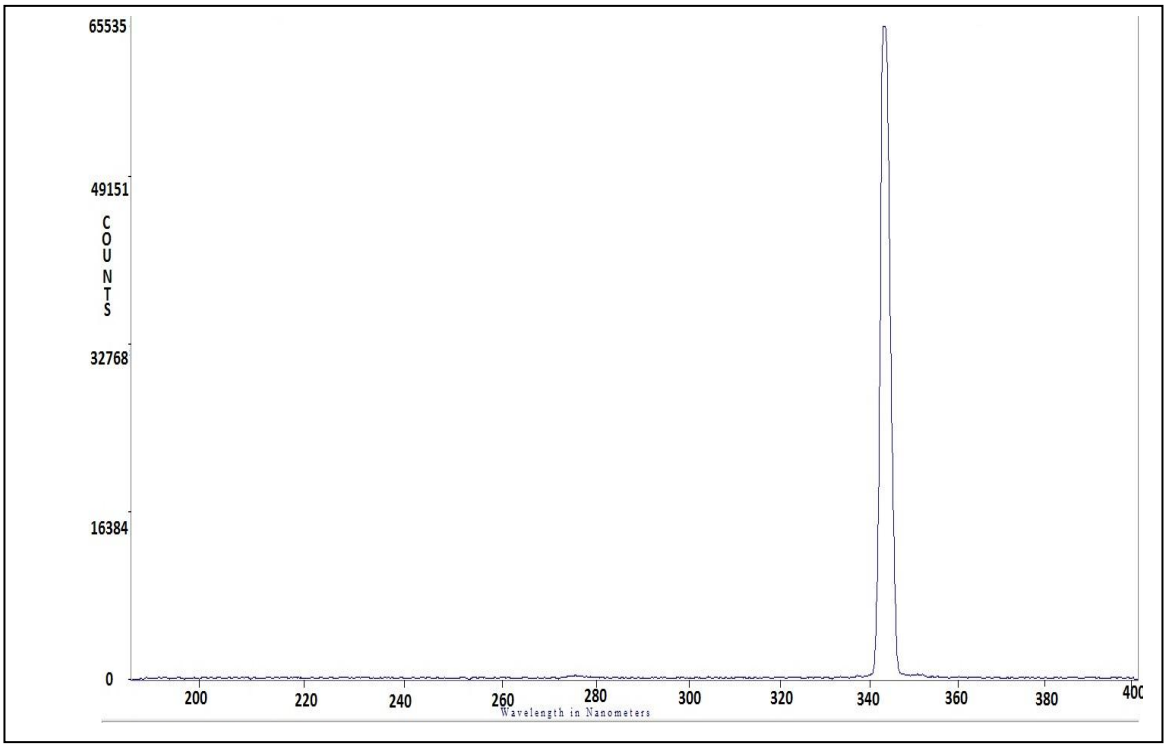

Figure (3.28): Emission line spectra (λ = 345 nm

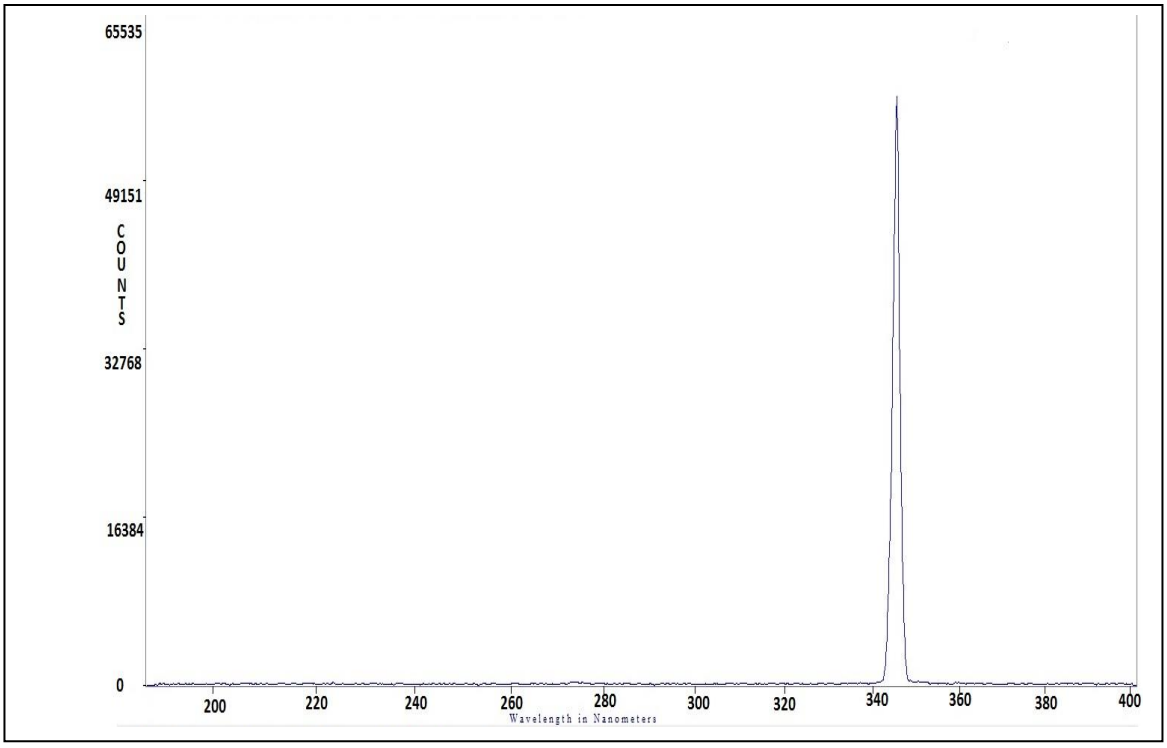

Figure (3.29): Emission line spectra at 346 nm

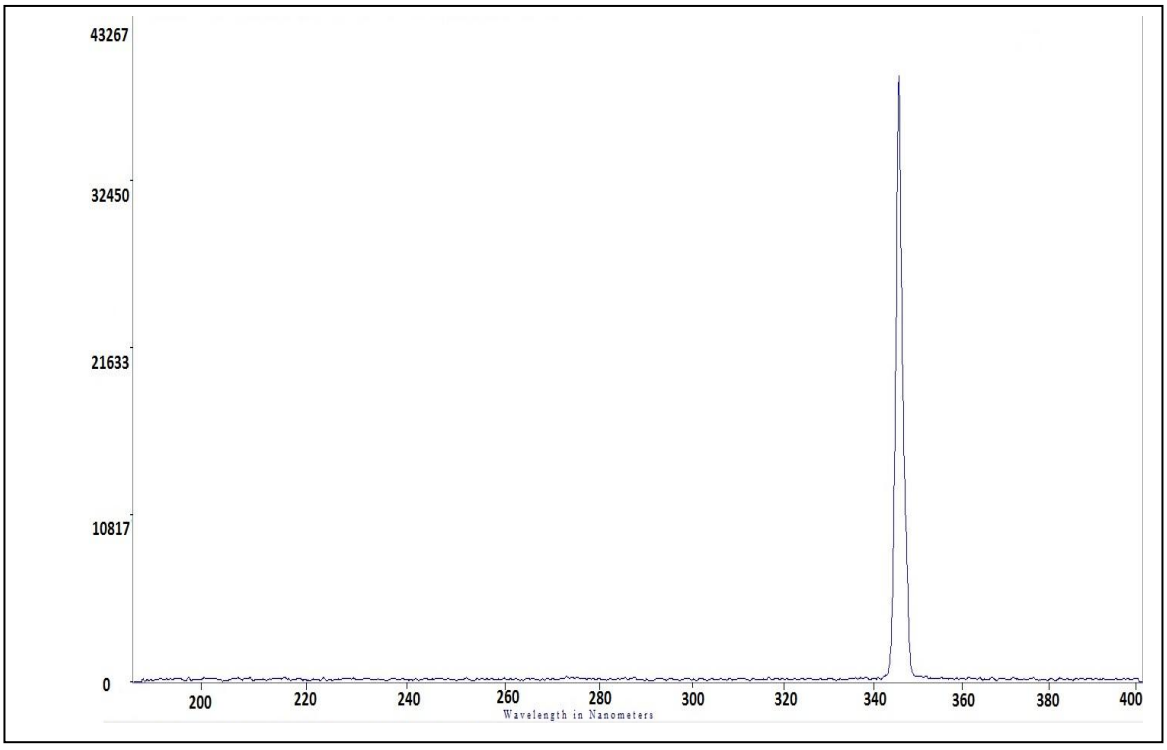

Figure (3.30): Emission line spectra at 347 nm

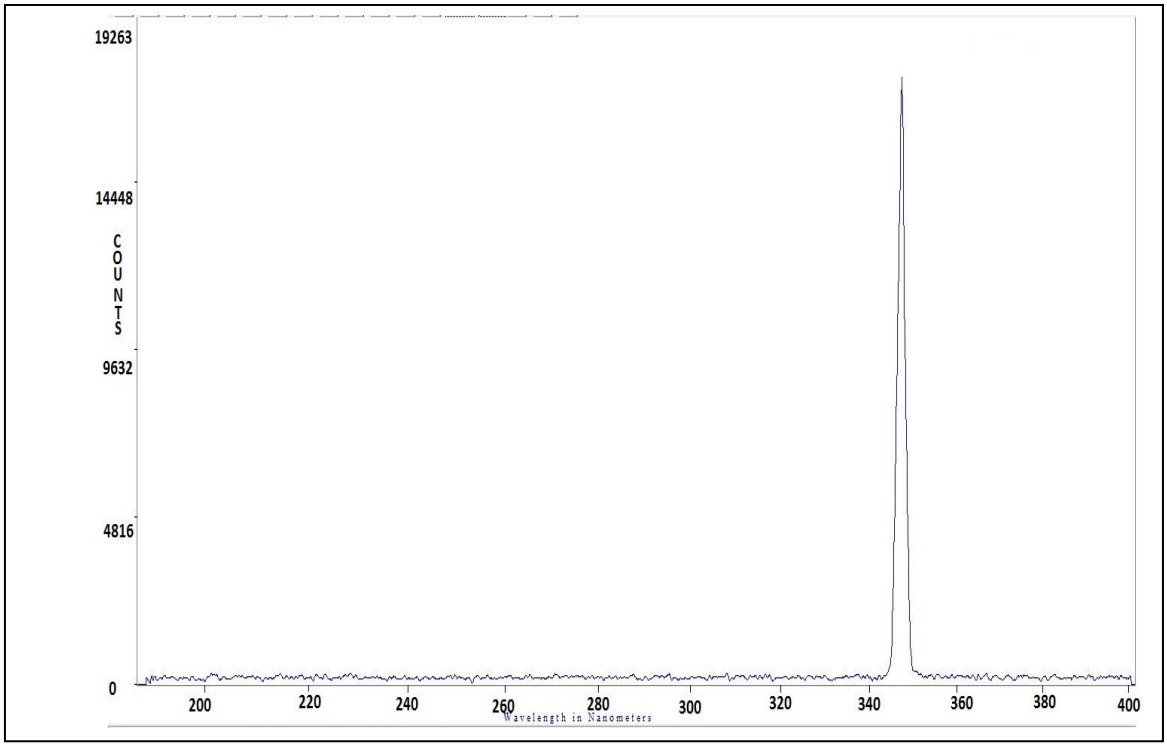

Figure (3.31): Emission line spectra at 348 nm

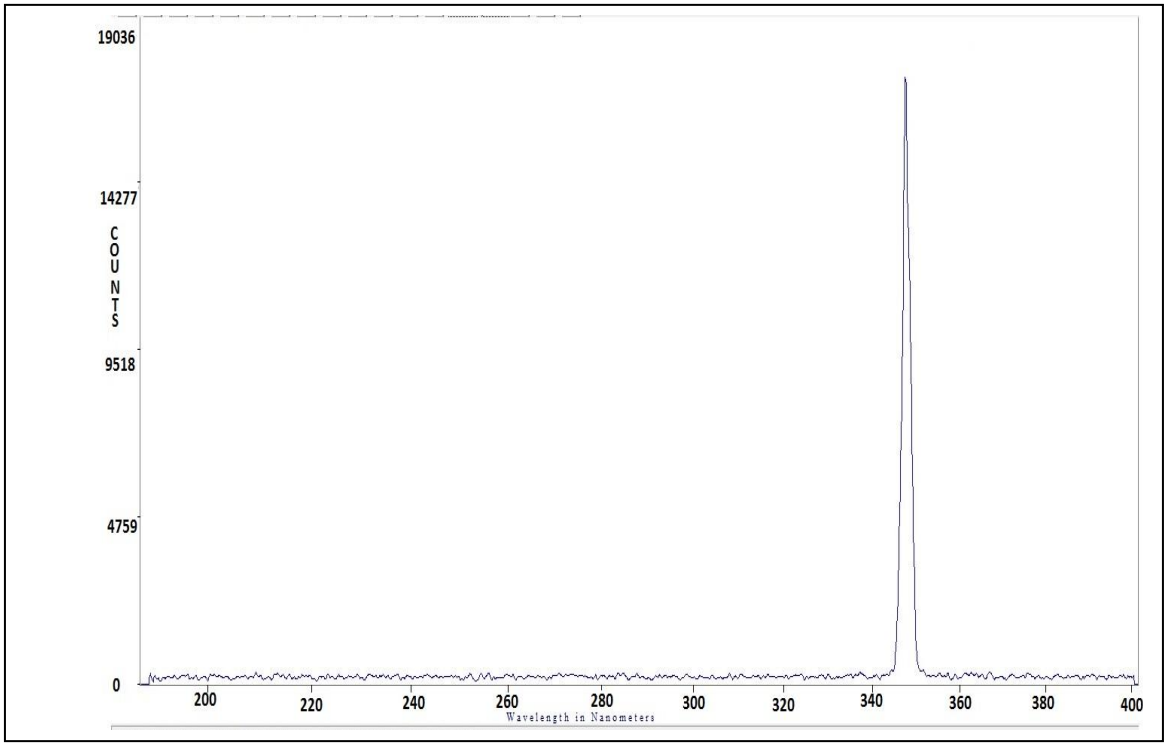

Figure (3.32): Emission line spectra at 349 nm

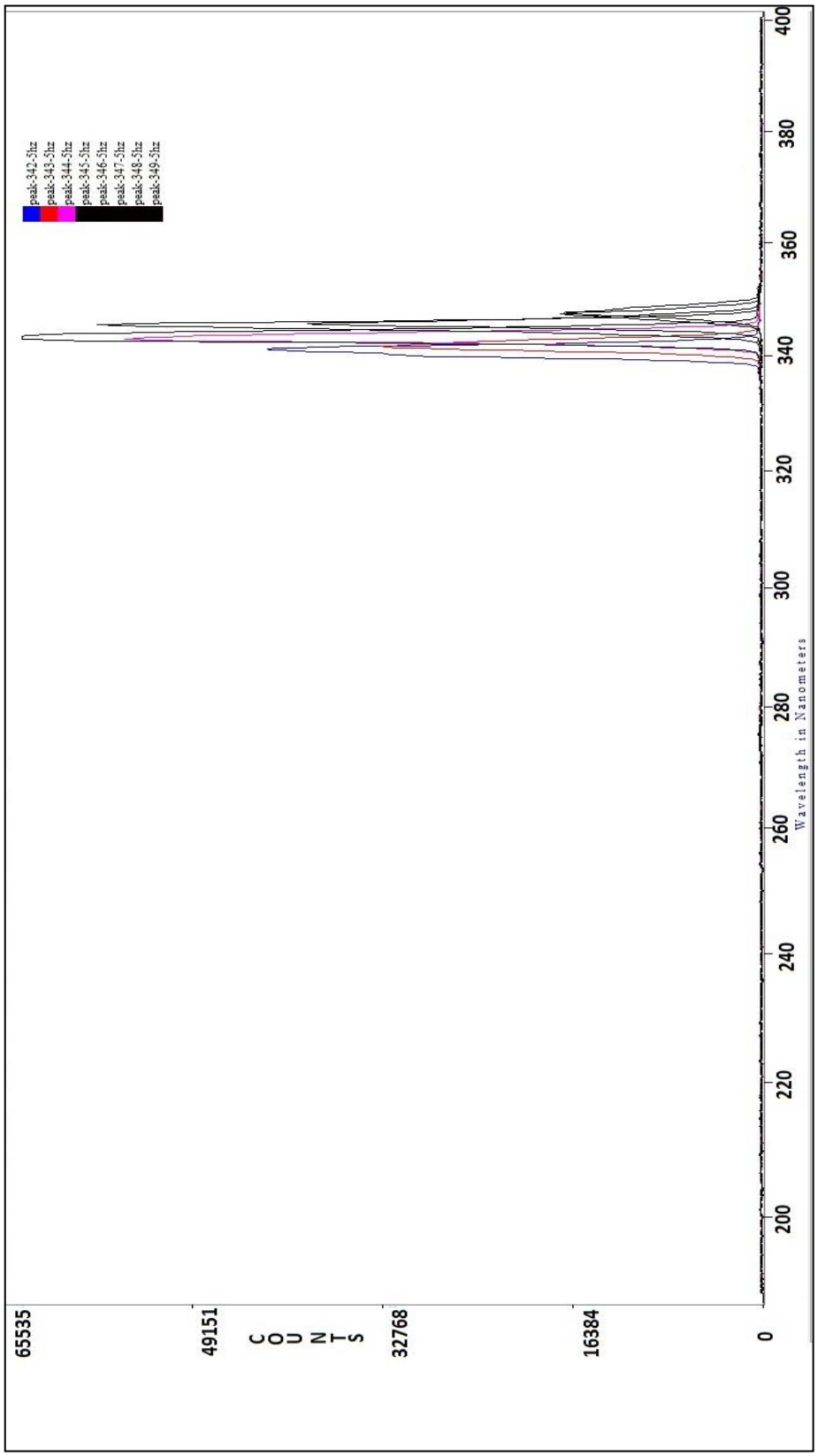

Figure (3.33): Collected emission spectra of laser induced holmium plasma with 650 mJ laser energy and (5Hz) repetition rate.

The result of figure (3.33) showing the collection of individual emission line from the spectral range (342-349) nm.

It has been approved that the maximum intensity of emission spectra was at 345 nm, for laser parameter of 650 mJ energy and 5Hz repetition rate .

3-2-6 Measuring the Individual of Holmium Emission Line Energy

Table (3.2) represents the energy of holmium emission line spectra for each nanometer for the range of 342nm to 349nm.

Table (3.2): Energy of holmium emission line

Wavelength (nm)	Energy of emission (μJ)
342	132
343	129
344	145
345	153
346	146
347	144
348	128
349	117

In table (3.2) it has been observed that the maximum energy was 153 μJ at λ= 345nm

3.2.7 Computational Results

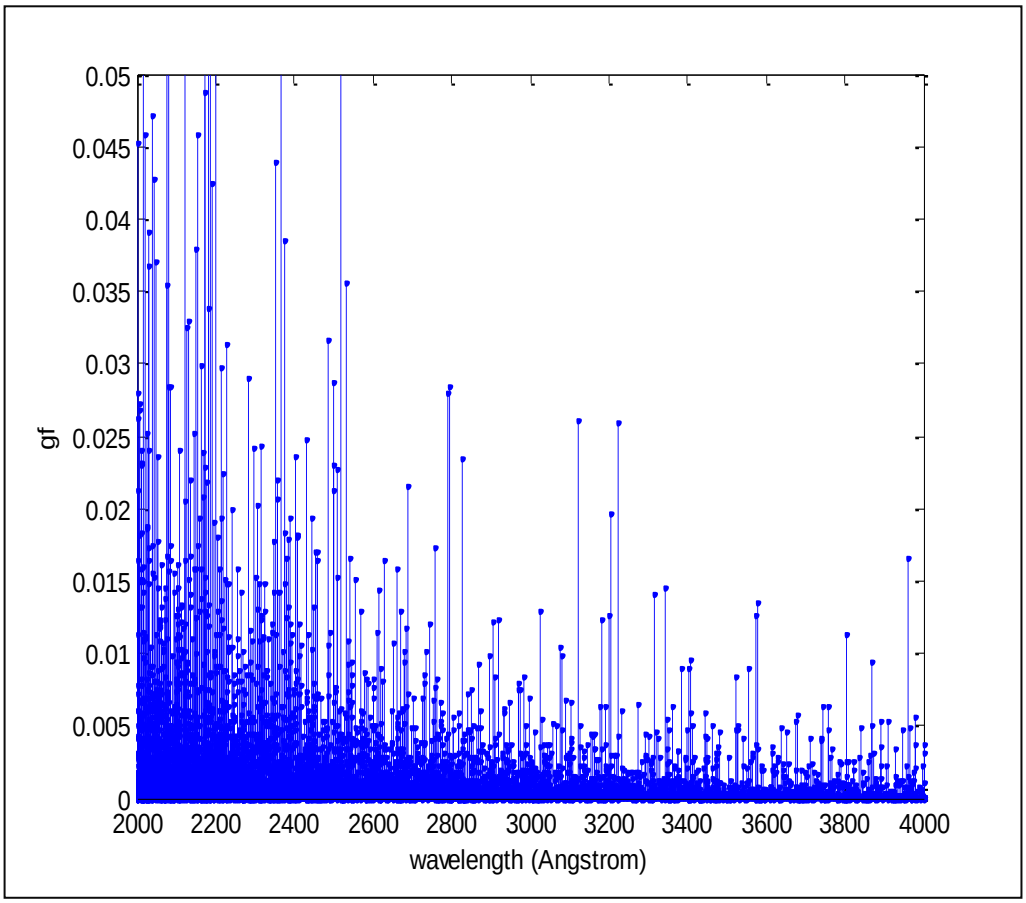

Figure (3.34): Emission spectra of the first ionization of (Ho II)

Figure (3.34) represents the emission spectra for Ho II (Dy like) ion. The first ionization stage of (Ho) is theoretically computed using Cowan code covering wavelength region between 200 to 400 nm. From computational method it has been illustrated that the emission spectra at λ= 345.75 nm is coming from from transition (4f)-5d.

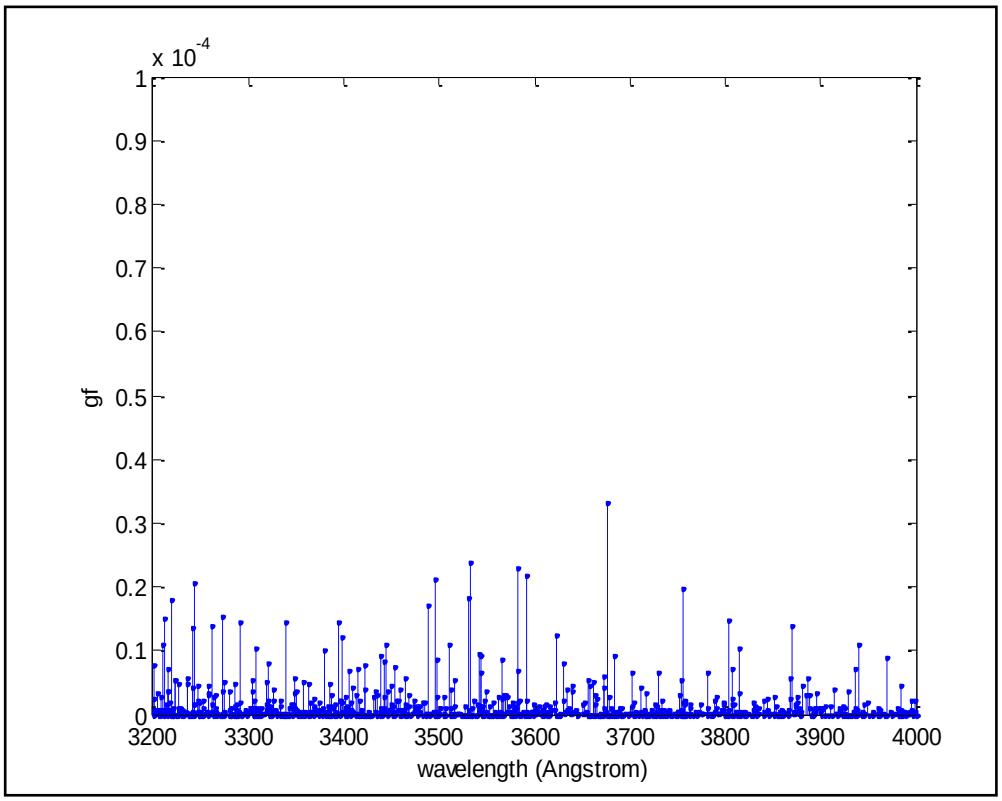

Figure (3.35): Emission spectra of the second ionization of (Ho III)

The emission spectra from Ho III (Tb like) ion, which is shown in figure (3.36) illustrates the second ionization stage of (Ho). Cowan code was used to cover wavelength region between (320 to 400) nm. From computational method, it has been observed that the emission spectra at (λ = 341.54 nm, and 345.64 nm) are coming from transition (4f)- 5d, while the emission spectra at λ= 342.76 nm is from (4p)-5d transition, and λ=345.53 nm it has been assigned transition from (4d)-5d.

3.3 Conclusion

From the previous expremantial and theoretical work for the investigated holmium emission spectra, one concludes the following.

1- The spectral line intensities produced from laser induced plasma emission exhibited a strong dependence on pulsed laser energy and repetition rate.

2- The maximum line emission intensity appeared at (λ= 341.54nm, 342.76nm and 345.53nm) respectively with the maximum intensity at (80000), when the repetition rate (20 Hz) and (800 mJ) laser pulse energy.

3- New maximum line emission intensity appeared at ג = 345.64nm when laser pulse energy 800 mJ and 10 Hz repetition rate was used.

4- The maximum emission intensity for each individual emission for each line from λ = 342 nm to 349 was 65535 at ג = 345 nm with laser energy 650 mJ and 5Hz repetition rate.

5- The energy of holmium emission line from λ = 342 nm to 349 nm with laser energy 650 mJ and 5Hz repetition rate shows, the maximum energy of line emission was 153μJ at ג = 345 nm.

6- From the theoretical calculation, for the first ionization stage of (Ho), it has been found that the emission line spectra at λ= 345.75 nm is coming from transition (4f)-5d. The second ionization stage of (Ho), it has been observed that the emission spectra at (λ = 341.54 nm, and 345.64 nm) respectively are coming from transition (4f)-5d, while the emission spectra at λ= 342.76 nm is from (4p)-5d transition, and λ=345.53 nm it has been assigned transition from (4d)-5d.

3.4 Future work

Many points can be taken in consideration to improve this work and get more suitable results. These points are:

1- Selecting different materials to study the emission spectra for each one in details and trying to find another emission sources in the UV regions in vacuum .

2- Using different laser wavelengths and study the effect of these wavelengths on the emission spectra.

3- Choosing different laser power densities and different laser pulse widths and trying to find the optimum parameters to produce the desired emission spectrum.

4- Using different laser energies to study the effect on the plasma emission at holmium target in vacuum and compared the result with plasma emission in air .

Reference

1. K. Miyamoto, "Controlled fusion and plasma physics", CRC Press (2006).
2. R. J. Goldston, and P. H. Rutherford, "Introduction to plasma physics", CRC Press (1995).
3. M. Z. Balbag, "Views of Prospective Science Teachers on Including the Concept of Plasma in Science Curricula", International Journal of Instruction. 11(2), 569-584 (2018).
4. K. Wiesemann, "A short introduction to plasma physics", arXiv preprint arXiv. 1404.0509 (2014).
5. P. M. Bellan, "Fundamentals of plasma physics", Cambridge University Press (2008).
6. P. Gibbon, "Introduction to Plasma Physics", arXiv preprint arXiv,1705.10529 (2017).
7. P. K. Carroll, and E. T. Kennedy, "Laser-produced plasmas". Contemporary Physics, 22(1), 61-96 (1981).
8. I. F. Rymdfysik, "Numerical Studies of Spacecraft-Plasma Interaction", Simulations of Wake Effects on the Cluster Electric Field Instrument EFW (2004).
9. E. V. Stenson, J. Horn-Stanja, M. R. Stoneking, and T. S.Pedersen, "Debye length and plasma skin depth: two length scales of interest in the creation and diagnosis of laboratory pair plasmas", Journal of Plasma Physics. 83(1) (2017).
10. M. V. Allmen and A. Blatter, "Laser-Beam Interaction with Materials", Springer, New York (1995).
11. G.P. Karman , McDonald GS, New GHC and Woerdman JP, Natur. 402:138 (1999).

12. T. Auguste, P. Monot, L. A. Lompré, G.Mainfray, and C. Manus, "Defocusing effects of a picosecond terawatt laser pulse in an underdense plasma", Optics communications. 89(2-4), 145-148 (1992).
13. P. W. Smorenburg, J. H. M. Kanters, A. Lassise, G. J. H. Brussaard, , L. P. J. Kamp, and O. J. Luiten, "Polarization-dependent ponderomotive gradient force in a standing wave", Physical Review A. 83(6), 063810 (2011).
14. T. Tajima, and J. M. Dawson, "Laser electron accelerator", Physical Review Letters. 43(4), 267 (1979).
15. C. D. Murphy, R. Trines, J. Vieira, A. J. W. Reitsma, R. Bingham, J. L. Collier, and P. A. Norreys, "Evidence of photon acceleration by laser wake fields", Physics of Plasmas. 13(3), 033108 (2006).
16. H. S. Brandi, C. Manus, G. Mainfray, T. Lehner, and G. Bonnaud, "Relativistic and ponderomotive self-focusing of a laser beam in a radially inhomogeneous plasma", I. Paraxial approximation. Physics of Fluids B: Plasma Physics. 5(10), 3539-3550 (1993).
17. H. Hora, "Theory of relativistic self-focusing of laser radiation in plasmas", JOSA. 65(8), 882-886 (1975).
18. M. Drescher, M.Hentschel, R. Kienberger, M. Uiberacker, V.Yakovlev, A. Scrinzi, and F.Krausz, "Time-resolved atomic inner-shell spectroscopy", Nature. 419(6909), 803(2002).
19. S.Kumar, P. K.Gupta, R. K. Singh, S. Sharma, R. Uma, and R. P. Sharma, "Pulse-compression and self-focusing of Gaussian laser pulses in plasma having relativistic–ponderomotive nonlinearity", Laser and Particle Beams. 35(3), 429-436 (2017).
20. S. A. Akhmanov, A. P. Sukhorukov, and R. V. Khokhlov, "Self-focusing and diffraction of light in a nonlinear medium", Soviet physics Uspekhi. 10(5), 609 (1968).

21. J. L. Shohet, "Encyclopedia of Plasma Technology", (Boca Raton, FL: CRC Press) (2016).
22. G. J. Tallents, "The physics of soft x-ray lasers pumped by electron collisions in laser plasmas", Journal of Physics D: Applied Physics. 36(15), R259 (2003).
23. D. Giulietti, and L.A. Gizzi, "X-ray emission from laser-produced plasmas", LaRivista del Nuovo Cimento, vol. 21, number 10 (1998).
24. A. De Giacomo, M. Dell'Aglio, R. Gaudiuso, S. Amoruso, and O. De Pascale," Effects of the background environment on formation, evolution and emission spectra of laser-induced plasmas", Spectrochim. Acta B. **78** 1(2012).
25. D. W. Hahn, and N. Omenetto, "Laser-induced breakdown spectroscopy (LIBS), part I: review of basic diagnostics and plasma–particle interactions: still-challenging issues within the analytical plasma community". Applied spectroscopy. 64(12), 335A-366A (2010).
26. F. Anabitarte, A. Cobo, and J. M. Lopez-Higuera, "Laser-induced breakdown spectroscopy: fundamentals, applications, and challenges", ISRN Spectroscopy (2012).
27. V. Majidi, and M. R. Joseph, "Spectroscopic applications of laser-induced plasmas", Critical Reviews in Analytical Chemistry, 23(3), 143-162 (1992).
28. M. B. Hooper, "Laser-Plasma Interactions 4", (Vol. 35). CRC Press (1989).
29. D. Salzmann, "Atomic physics in hot plasmas ", (Vol. 97). Oxford University Press on Demand (1998).
30. K. Chaudhary, S. Z. H. Rizvi, and J.Ali, "Laser-induced plasma and its applications. In Plasma Science and Technology-Progress in Physical States and Chemical Reactions". InTech (2016).

31. P. Moroshkin, and K. Kono, "Bound-bound transitions in the emission spectra of Ba+-He excimer", Physical Review A, 93(5), 052510 (2016).

32. A. W .Sáenz, A. Nagl, and H. Überall, "Calculation of free-bound transition strength in channeling radiation or coherent bremsstrahlung", Nuclear Instruments and Methods in Physics Research Section B: Beam Interactions with Materials and Atoms, 13(1-3), 23-26 (1986).

33. M. J. Seaton, "Free-free transitions and spectral-line broadening", Journal of Physics B: Atomic, Molecular and Optical Physics. 33(14), 2677 (2000).

34. A. P. Thorne , "Spectrophysics", 1st Edition. London, 1974.

35. R. D. Hazeltine, "The framework of plasma physics", CRC Press (2018).

36. J. Hermann, D. Grojo, E. Axente, and V. Craciun, "Local thermodynamic equilibrium in a laser-induced plasma evidenced by blackbody radiation", Spectrochimica Acta Part B: Atomic Spectroscopy. 144, 82-86 (2018).

37. G. Cristoforetti, , A. De Giacomo, M. Dell'Aglio, S. Legnaioli, E. Tognoni, V. Palleschi, and N. Omenetto, "Local thermodynamic equilibrium in laser-induced breakdown spectroscopy: beyond the McWhirter criterion", Spectrochimica Acta Part B: Atomic Spectroscopy. 65(1), 86-95 (2010).

38. V. Morel, and A. Bultel, "Achievement of local thermodynamic equilibrium for ns laser-induced plasmas on aluminium sample at different wavelengths", In Journal of Physics: Conference Series (Vol. 550, No. 1, p. 012048). IOP Publishing (2014).

39. M. Baeva, , D. Uhrlandt, and A. B.Murphy," A collisional-radiative model

of iron vapour in a thermal arc plasma", Journal of Physics D: Applied Physics. 50(22), 22LT02 (2017).

40. D. A Cremers, and L. J. Radziemski, "Handbook of laser-induced breakdown spectroscopy", John Wiley & Sons (2013).
41. S. Eliezer, "The interaction of high-power lasers with plasmas", CRC press (2002).
42. H. R. Griem, "Plasma Spectroscopy", Mc-Grew-Hill Book Company, New York (1964).
43. M. Konuma, "Film deposition by plasma techniques", Springer Science & Business Media (Vol. 10) (2012).
44. A. Fridman, and L. A. Kennedy, "Plasma physics and engineering". CRC press (2004).
45. C. Müller, H. Hu, B. Najjari, J. C. López-Urrutia, Z.Harman, and A. B. Voitkiv, "Electron recombination in dense photonic, electronic and atomic environments", In Journal of Physics: Conference Series (Vol. 388, No. 1, p. 012003). IOP Publishing (2012).
46. C. V. Bindhu, S. S. Harilal, M. S. Tillack, , F. Najmabadi, and A. C.Gaeris, "Energy absorption and propagation in laser-created sparks", Applied spectroscopy. 58(6), 719-726 (2004).
47. J. Gunst, Y. Wu, C. H Keitel, and A. Pálffy, "Nuclear excitation by electron capture in optical-laser-generated plasmas", Physical Review E, 97(6), 063205 (2018).
48. S. S. Harilal, C. V. Bindhu, M. S. Tillack, F. Najmabadi,and A. C. Gaeris, "Internal structure and expansion dynamics of laser ablation plumes into ambient gases", Journal of Applied Physics. 93(5), 2380-2388 (2003).
49. F. Garrelie, J. Aubreton, and A. Catherinot, "Monte Carlo simulation of the laser-induced plasma plume expansion under vacuum: Comparison

with experiments", Journal of applied physics. 83(10), 5075-5082 (1998)..

50. V. N. Rai, and S. N. Thakur, "Physics of plasma in laser-induced breakdown spectroscopy", In Laser-Induced Breakdown Spectroscopy (pp. 83-111). Elsevier (2007)..
51. Y. Okano, Y. Hironaka, K. G. Nakamura, and K. I. Kondo, "Time-resolved electron shadowgraphy for 300 ps laser ablation of a copper film", Applied physics letters, 83(8), 1536-1538 (2003)..
52. J. P. Singh, and S. N. Thakur, "Laser-induced breakdown spectroscopy", Elsevier (2007). .
53. Y. P. Raizer, "Physics of shock waves and high-temperature hydrodynamic phenomena", Courier Corporation (2002).
54. A. Semerok,and C. Dutouquet, "Ultrashort double pulse laser ablation of metals", Thin solid films, 453, 501-505 (2004).
55. R. d'Agostino, , P. Favia, , C. Oehr, and , M. R Wertheimer, "Low-temperature plasma processing of materials: past, present, and future", Plasma Processes and Polymers. 2(1), 7-15 (2005).
56. A. W. Miziolek, V. Palleschi, and I. Schechter, "Laser induced breakdown spectroscopy", Cambridge university press (2006).
57. B. Cagnac, and J. C. Pebay-Peyroula, "Modern atomic physics: fundamental principles", (1975).
58. L. Fechner, "High-Resolution Experiments on Strong-Field Ionization of Atoms and Molecules: Test of Tunneling Theory, the Role of Doubly Excited States, and Channel-Selective Electron Spectra", Springer (2016).
59. A. Ciucci, V. Palleschi, S. Rastelli, R. Barbini, F. Colao, R.Fantoni,and H. J. L. Van der Steen, "Trace pollutants analysis in soil by a time-

resolved laser-induced breakdown spectroscopy technique" Applied Physics B, 63(2), 185-190 (1996).

60. D. Bulajic, M. Corsi, G. Cristoforetti, S. Legnaioli, V. Palleschi, A. Salvetti, and E. Tognoni, "A procedure for correcting self-absorption in calibration free-laserinduced breakdown spectroscopy", Spectrochimica Acta Part B: Atomic Spectroscopy. 57(2), 339-353 (2002).
61. M. Corsi, G. Cristoforetti, M. Hidalgo, S. Legnaioli, V. Palleschi, A. Salvetti, and C. Vallebona, "Double pulse, calibration-free laser-induced breakdown spectroscopy: a new technique for in situ standard-less analysis of polluted soils", Applied Geochemistry. 21(5), 748-755 (2006).
62. M. G. Kompitsas, F. Roubani-Kalantzopoulou, I. Bassiotis, , A. Diamantopoulou, and A. Giannoudakos, "Laser induced plasma spectroscopy (LIPS) as an efficient method for elemental analysis of environmental samples", EARSeL Proceedings No. 1 (2000).
63. B. C. Castle, K. Talabardon, B. W. Smith, and J. D. Winefordner, "Variables influencing the precision of laser-induced breakdown spectroscopy measurements", Applied Spectroscopy. 52(5), 649-657 (1998).
64. S. Eliezer, and Y. Eliezer, "The fourth state of matter: an introduction to plasma science", CRC Press (2001).
65. T. D Hettipathirana, and M. W. Blades, "Furnace atomization plasma excitation spectroscopy: spectral, spatial, and temporal characteristics", Spectrochimica Acta Part B: Atomic Spectroscopy. 47(4), 493-503 (1992).
66. B. Charles, and K. J. Fredeen, "Concepts, instrumentation and techniques in inductively coupled plasma optical emission spectrometry", Perkin Elmer Corporation (1997).

67. S. S. Harilal, R. C. Issac, C. V. Bindhu, V. P. N. Nampoori, and , C. P. G. Vallabhan, "Optical emission studies of species in laser-produced plasma from carbon", Journal of Physics D: Applied Physics. 30(12), 1703 (1997).

68. Y. L. Chen, J. W. L. Lewis, and C. Parigger, Spatial and temporal pro" les of pulsed laser-induced air plasma emissions (1998).

69. B. Le Drogoff, J. Margot, M. Chaker, M. Sabsabi, O. Barthelemy, T. W. Johnston, and Y. Von Kaenel, "Temporal characterization of femtosecond laser pulses induced plasma for spectrochemical analysis of aluminum alloys", Spectrochimica acta part B: Atomic spectroscopy, 56(6), 987-1002 (2001).

70. V. N Rai, J. P. Singh, F. Y. Yueh, and R. L. Cook, "Study of optical emission from laser-produced plasma expanding across an external magnetic field". Laser and Particle Beams. 21(1), 65-71 (2003).

71. S. S. Harilal, B. O'Shay, M. S. Tillack, and M. V. Mathew, "Spectroscopic characterization of laser-induced tin plasma. Journal of applied physics", 98(1), 013306 (2005).

72. N. M Shaikh, S. Hafeez, B. Rashid, and M. A. Baig, "Spectroscopic studies of laser induced aluminum plasma using fundamental, second and third harmonics of Nd: YAG laser", The European Physical Journal D. 44(2), 371-379 (2007).

73. A. Elhassan, A. Giakoumaki, D. Anglos, G. M. Ingo, L. Robbiola, and M. A. Harith, "Nanosecond and femtosecond laser induced breakdown spectroscopic analysis of bronze alloys". Spectrochimica Acta Part B: Atomic Spectroscopy. 63(4), 504-511 (2008).

74. R. W. Coons, S. S. Harilal, M. Polek, and A. Hassanein, "Spatial and temporal variations of electron temperatures and densities from EUV-

emitting lithium plasmas". Analytical and bioanalytical chemistry. 400(10), 3239-3246 (2011).

75. M. Hanif, , M.Salik, and M. A. Baig, "Optical spectroscopic studies of titanium plasma produced by an Nd: YAG laser",Optics and Spectroscopy. 114(1), 7-14 (2013).
76. H. Hegazy, E. AlAshkar, , H. H. Abou-Gabal, , M. N. Aly, and N. Hamed, "Spectroscopic Evolution of Plasma Produced by Nd-YAG Laser. IEEE Transactions on Plasma Science. 42(6), 1674-1684 (2014).
77. M. Hanif, and M. Salik, "Optical emission characterization of laser ablated zirconium plasma", Optics and Spectroscopy. 118(4), 631-638 (2015).
78. J. Hou, L.Zhang, W. Yin, Y. Zhao, W. Ma, L. Dong, and S. Jia, "Investigation on spatial distribution of optically thin condition in laser-induced aluminum plasma and its relationship with temporal evolution of plasma characteristics", Journal of Analytical Atomic Spectrometry.32(8), 1519-1526 (2017).
79. F. Torretti, R. Schupp, D. Kurilovich, A. Bayerle, J. Scheers, , W. Ubachs, and O. O. Versolato, "Short-wavelength out-of-band EUV emission from Sn laser-produced plasma", Journal of Physics B: Atomic, Molecular and Optical Physics. 51(4), 045005 (2018).
80. Q. A. Abbas, "Effect of Target properties on the Plasma Characteristics that produced by Laser at Atmospheric Pressure", Iraqi Journal of Science. 60(6), 1251-1258 (2019).
81. G. Başar, N. Al-Labady, B. Özdalgiç, F. Güzelçimen, A. Er, I. K.Öztürk, and S. Kröger, "Line Identification of Atomic and Ionic Spectra of Holmium in the Near-UV. II. Spectra of Ho ii and Ho iii". The Astrophysical Journal Supplement Series, 228(2), 17(2017).

82. Cowan, (1968). Theoretical calculation of atomic spectra using digital computers. JOSA, 58(6), 808-818.

83. R. D. Cowan, "The theory of atomic structure and spectra (No. 3)", Univ of California Press, (1981) .

84. M. Kuzuya, H. Matsumoto, H.Takechi, and O. Mikami, "Effect of Laser Energy on Spectral Emission from a Plasma Induced by a Q-switched Nd Laser in Different Atmospheres", Journal of the Spectroscopical Society of Japan. 41(5), 327-331(1992).

85. H. Legall, C. Schwanke, J. Bonse, and J. Krüger, "The influence of processing parameters on X-ray emission during ultra-short pulse laser machining", Applied Physics A, 125(8), 570 (2019).

86. H. H. Murbat, and H. A. Hamza,. " The Influence of Nd: YAG Laser Energy on Plasma Characteristics Produced on Si: Al Alloy Target in Atmosphere Pressure". Journal of Materials Sciences and Applications. 1(1), 1(2017).

الخلاصة

في هذا البحث تمت دراسة طيف الهولميوم المنبعث من البلازما المتولده بليزر النيديميوم - ياك ذوعامل النوعيه Q-Switched والطول الموجي ١٠٦٤ نانومتر في المنطقة الطيفية (٢٠٠-٤٠٠) نانومتر. تم استخدام طاقات مختلفة من نبضات الليزر (٦٠٠ ، ٦٥٠ ، ٧٠٠ ، ٧٥٠ ، ٨٠٠) ملي جول مع ترددات (١هرتز، ٥ هرتز، ١٠ هرتز، ٢٠ هرتز). تمت دراسة تأثير طاقة نبضة الليزر مع التردد على شدة الانبعاثات الطيفية للبلازما المنتجة بالليزر باستخدام التقنية الطيفية في (الضغط الجوي الاعتيادي) .

تظهر أفضل أطياف الانبعاث عندما تكون طاقة نبضة الليزر ٨٠٠ مللي جول بتردد ٢٠ هرتز عند الاطوال الموجية (٣٤٥,٥٣و ٣٤٢,٧٦ و٣٤١,٥٤) نانومتر على التوالي ، مع أقصى شدة تبلغ ٨٠٠٠٠ .

تمت دراسة شدة الانبعاثات الطيفية للهولميوم لكل طول موجي في المنطقة الطيفية (٣٤٢ الى ٣٤٩) نانومتر عندما تكون طاقة نبضة الليزر ٦٥٠ ملي جول وتردد ٥ هرتز وشدة اقوى انبعاث طيفي كانت ٦٥٥٣٥ عند الطول الموجي ٣٤٥ نانومتر.

كذلك تم التحقق من طاقة الانبعاثات الطيفية لكل طول موجي للمنطقة الطيفية (٣٤٢ الى ٣٤٩) نانومتر بطاقة نبضة الليزر ٦٥٠ ملي جول وتردد ٥ هرتز وكانت الطاقة القصوى لطيف الانبعاث الخطي ١٥٣ مايكرو جول عند الطول الموجي ٣٤٥ نانومتر.

تم استخدام برنامج (Cowan) في المحاكاة النظرية لدراسة الانتقالات الاكترونية للبلازما المتولده من الهولميوم. تشير النتائج إلى أن شدة الانبعاثات تزداد بزيادة طاقة النبضه الليزرية و التردد.

جمهورية العراق

وزارة التعليم العالي والبحث العلمي

جامعة بغداد

معهد الليزر للدراسات العليا

خصائص الانبعاث الطيفي للهولميوم في المنطقة الطيفية (٢٠٠-٤٠٠) نانومتر

رسالة مقدمة الى

معهد الليزر للدراسات العليا / جامعة بغداد / لاستكمال متطلبات شهادة ماجستير علوم في الليزر / الفيزياء

من قبل

نبراس نزيه محمود

بكالوريوس علوم فيزياء الليزر -٢٠٠٢

بإشراف

المدرس الدكتور محمود شاكر محمود

١٤٤١ هـ ٢٠٢٠ م